

Three-level atom laser model with results and applications

A. M. Smith and C. W. Gardiner

Department of Physics, University of Waikato, Hamilton, New Zealand

(Received 12 December 1988; revised manuscript received 11 October 1989)

We present here a fully quantum-mechanical treatment of the laser using a three-level atom model. The phase-space method employed is identical to that in a previous publication of ours [Phys. Rev. A **38**, 4073 (1988)] and again results in a Fokker-Planck description of the laser without any approximations. The third level only provides extra deterministic terms and, if it is regarded as a further reservoir to the lasing levels, then the resultant stochastic equations have much improved stability. These equations are suitable for extensive theoretical analysis of both the laser and optical bistability, although in this paper we have concentrated on the adiabatically eliminated limit and calculated the leading noise terms in various regimes. However, we do use the technique of direct numerical simulation to solve exactly the full system of laser equations. The results display clearly many of the known laser characteristics.

I. INTRODUCTION

In a previous paper,¹ we introduced a phase-space method for the laser involving two-level atoms, resulting in a Fokker-Planck equation which described the system without a truncation of higher-order derivatives. However, a consequence of this method was a stochastic equation for an extra variable, the moments of which were equal to those of the total number of atoms, but with an additional source of noise variation. This noise had no immediate physical interpretation and prevented the use of standard techniques for the solution of the system.

The purpose of this present work, then, is to investigate a more realistic Fokker-Planck equation for the laser, which while maintaining the desirable properties of our previous equation, now contains further deterministic terms to stabilize the extra stochastic equation. This is achieved by considering another model for the laser consisting of an ensemble of three-level atoms which interact via the upper two levels with a single mode inside a cavity. Using the same approach and method generalized from the two-level model, a characteristic function equation and then Fokker-Planck equation may be derived for the system. Under the reasonable assumption, first introduced by Gordon,² that the ground level may be treated as an extra reservoir to the lasing levels, we obtain stable stochastic equations which describe the operation of the laser and optical bistability, under completely general conditions.

The course of this paper is as follows. Sect. II introduces the Hamiltonian model and master equation for the three-level system, which is familiar from other research.³ We now define extra raising and lowering operators to describe the extra possible transitions to and from the third level. The procedure is equivalent to that for the two-level model, except that the matrices defined are 3×3 matrices and a new algebra has to be defined. The master equation is then written in terms of these operator matrices.

In Sec. III we introduce the three-level characteristic function, in a similar fashion to that developed in Ref. 1. The atomic part is again written as a linear combination of the atomic operators, but we now require five variables to obtain a closed set with the new master equation. Using the new operator algebra we derive a differential equation for the characteristic equation.

Using techniques based on the positive P representation of Drummond and Gardiner⁴ in Sec. IV, we next convert the characteristic function equation into a Fokker-Planck equation involving classical variables in phase space. This Fokker-Planck equation has positive semidefinite diffusion and is obtained without the truncation of higher-order derivatives required in traditional phase-space methods. A set of seven corresponding stochastic differential equations may then be inferred. The equation for the number of atoms in the lasing levels has now been stabilized, but at the expense of an unexplained variation in a variable with moments equal to those of the total number of three-level atoms.

In Sec. V we consider the various models for laser operation allowed by a three-level atomic system. The first of these results in essentially a correction to the two-level equations, but in addition we consider models in which the extra level transitions are fundamental in producing the population inversions. Following Gordon, we then assume that there is effectively an infinite number of atoms in the ground level, which acts as an additional reservoir to the few atoms in the lasing levels. This allows us to consider again a six-equation system for the laser and optical bistability, but now with considerably improved stability properties.

We next introduce (Sec. VI) scaled variables, essentially equivalent to those considered by Carmichael, Satchell, and Sarkar,⁵ in order to more clearly reveal the physics in the equations. The scaled equations demonstrate that it is the size of the saturation photon number n_s which determines the size of the stochastic noise and hence whether the semiclassical predictions are likely to be correct.

In Sec. VII, for the adiabatic elimination limit, a simplified set of equations may be found for the cavity variables. The Fokker-Planck equation is complicated, but for large and small intensities the dominant noise terms may be determined. For the laser configuration, these are equivalent to those derived using the two-level system, but a new Fokker-Planck equation which may have an application in Jaynes-Cumming problems is also presented.

Finally, in Secs. VIII and IX, we use the powerful technique of numerical simulations and apply it to our full system of six equations in a laser configuration. The numerical scheme employed is the deterministically stable mixed implicit-explicit method of McNeil and Craig.⁶ This work represents the first serious attempt to simulate laser operation using the full set of phase-space equations. The results clearly display many of the known laser characteristics such as threshold, critical slowing down, and coherent light production above threshold. Although some numerical spiking is present at threshold, it does not appear to have the pathological consequences discovered in our recent work on numerical simulations.⁷

II. THREE-LEVEL ATOM LASER MODEL AND MASTER EQUATION

The model we shall consider is of an ensemble of N_T atoms coupled to a single mode inside a cavity. However, the atoms now have three levels 0,1,2 and are described by the operators $a_0, a_0^\dagger, a_1, a_1^\dagger, a_2, a_2^\dagger$ which obey the standard anticommutation relations

$$a_i^\dagger a_j + a_j a_i^\dagger = \delta_{ij}, \quad a_i a_j + a_j a_i = 0. \quad (2.1)$$

As is shown in Fig. 1, level 0 is taken as the ground level and defined to correspond to zero energy. The upper two levels are the lasing levels and are split by frequency ω about the excitation energy E . The cavity mode is described by the operators a and a^\dagger , with the frequency tuned to the resonance frequency ω , the atomic energy level difference.

In addition, the three-level atomic system is damped by a reservoir which can be used to provide the energy for level transitions. The cavity mode is also damped by a finite-temperature reservoir to represent losses through the cavity mirrors.

In the rotating-wave and electric dipole approximations, the Hamiltonian for this system is

$$\begin{aligned} H &= \sum_{i=0}^3 H_i, \\ H_0 &= \hbar\omega a^\dagger a + \hbar\omega \sum_{\mu=1}^{N_T} \frac{1}{2} ([a_2^\dagger a_2]_\mu - [a_1^\dagger a_1]_\mu) \\ &\quad + \hbar E \sum_{\mu=1}^{N_T} ([a_2^\dagger a_2]_\mu + [a_1^\dagger a_1]_\mu), \\ H_1 &= ig\hbar \sum_{\mu=1}^{N_T} (a^\dagger [a_1^\dagger a_2]_\mu - a [a_2^\dagger a_1]_\mu), \end{aligned} \quad (2.2)$$

with H_2 and H_3 representing Hamiltonian terms describ-

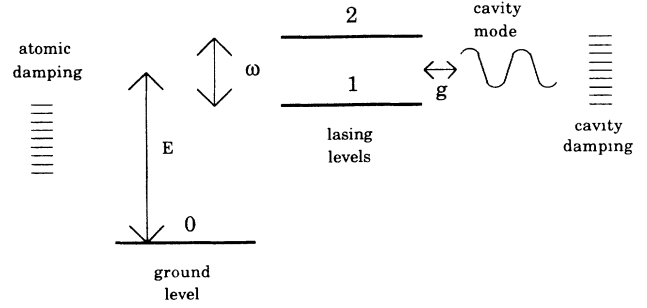


FIG. 1. Diagram of the three-level atom laser model.

ing the atomic and cavity damping. We now follow the standard techniques⁸ to write the corresponding master equation. In the interaction picture, using a reference frame which eliminates the free-energy Hamiltonian terms in H_0 , this is

$$\frac{\partial \rho}{\partial t} = \frac{1}{i\hbar} [H_1, \rho] + \left. \frac{\partial \rho}{\partial t} \right|_A + \left. \frac{\partial \rho}{\partial t} \right|_F, \quad (2.3)$$

$$\begin{aligned} \left. \frac{\partial \rho}{\partial t} \right|_F &= \kappa n (2a^\dagger \rho a - a a^\dagger \rho - \rho a a^\dagger) \\ &\quad + \kappa(n+1)(2a \rho a^\dagger - a^\dagger a \rho - \rho a^\dagger a) \\ &\quad - \kappa m (2a^\dagger \rho a^\dagger - a^\dagger a^\dagger \rho - \rho a^\dagger a^\dagger) \\ &\quad - \kappa m^* (2a \rho a - a a \rho - \rho a a), \end{aligned} \quad (2.4)$$

$$\begin{aligned} \left. \frac{\partial \rho}{\partial t} \right|_A &= \sum_{\mu=1}^{N_T} \sum_{i=0}^2 \sum_{j=0}^2 \frac{1}{2} \omega_{ij} (2[a_i a_j^\dagger]_\mu \rho [a_i^\dagger a_j]_\mu \\ &\quad - [a_i^\dagger a_j]_\mu [a_i a_j^\dagger]_\mu \rho \\ &\quad - \rho [a_i^\dagger a_j]_\mu [a_i a_j^\dagger]_\mu). \end{aligned} \quad (2.5)$$

The terms in (2.4) involving the parameters m and m^* are unconventional, and are included to allow the possibility of a squeezed bath. However, in all numerical work m and m^* will be set equal to zero.

The parameter κ gives the rate of energy loss of the cavity mode, principally through the mirrors. The atomic damping rates define two mechanisms; the first ω_{ij} , where $i \neq j$, gives the rate of transition from level i to level j by either pumping or emission (see Fig. 2) and the second ω_{ii} , allows for reservoir-induced random phase shifts and collisional broadening.

For the two-level atom system it has proved convenient to use the analogy with a spin- $\frac{1}{2}$ particle in a magnetic field. This involves the identification of the Fermi operators with the Pauli matrices as

$$\begin{aligned} [a_1^\dagger a_2]_\mu &= \sigma_\mu^-, \quad [a_2^\dagger a_1]_\mu = \sigma_\mu^+, \\ \frac{1}{2} [a_2^\dagger a_2 - a_1^\dagger a_1]_\mu &= \sigma_{\mu,z}, \quad [a_2^\dagger a_2 + a_1^\dagger a_1]_\mu = 1, \end{aligned} \quad (2.6)$$

where

$$\sigma_{\mu}^{-} = \begin{pmatrix} 0 & 1 \\ 0 & 0 \end{pmatrix},$$

$$\sigma_{\mu}^{+} = \begin{pmatrix} 0 & 0 \\ 1 & 0 \end{pmatrix},$$

$$\sigma_{\mu,z} = \frac{1}{2} \begin{pmatrix} -1 & 0 \\ 0 & 1 \end{pmatrix}.$$

The standard technique is to substitute the Pauli matrices into the two-level master equation and use their known algebra. The extension to three levels is similar and requires the definition of two new sets of raising and lowering operators

$$[a_1^{\dagger}a_0]_{\mu} = \chi_{\mu}^{+}, \quad [a_1a_0^{\dagger}]_{\mu} = \chi_{\mu}^{-}, \quad [a_2^{\dagger}a_0]_{\mu} = \phi_{\mu}^{+},$$

$$[a_2a_0^{\dagger}]_{\mu} = \phi_{\mu}^{-}. \quad (2.7)$$

It is then possible to define three-dimensional matrices, corresponding to the two-dimensional Pauli matrices, which include terms for all three levels

$$\sigma_{\mu}^{+} = \begin{pmatrix} 0 & 0 & 0 \\ 0 & 0 & 0 \\ 0 & 1 & 0 \end{pmatrix}, \quad \sigma_{\mu}^{-} = \begin{pmatrix} 0 & 0 & 0 \\ 0 & 0 & 1 \\ 0 & 0 & 0 \end{pmatrix},$$

$$\sigma_{\mu,z} = \frac{1}{2} \begin{pmatrix} 0 & 0 & 0 \\ 0 & -1 & 0 \\ 0 & 0 & 1 \end{pmatrix}, \quad \chi_{\mu}^{+} = \begin{pmatrix} 0 & 0 & 0 \\ 1 & 0 & 0 \\ 0 & 0 & 0 \end{pmatrix}, \quad (2.8)$$

$$\chi_{\mu}^{-} = \begin{pmatrix} 0 & 1 & 0 \\ 0 & 0 & 0 \\ 0 & 0 & 0 \end{pmatrix}, \quad \phi_{\mu}^{+} = \begin{pmatrix} 0 & 0 & 0 \\ 0 & 0 & 0 \\ 1 & 0 & 0 \end{pmatrix},$$

$$\phi_{\mu}^{-} = \begin{pmatrix} 0 & 0 & 1 \\ 0 & 0 & 0 \\ 0 & 0 & 0 \end{pmatrix}.$$

For completeness, we also require the two diagonal matrices

$$H_1 = ig\hbar \sum_{\mu=1}^{N_T} (a^{\dagger}\sigma_{\mu}^{-} - a\sigma_{\mu}^{+}), \quad (2.10)$$

$$\left. \frac{\partial \rho}{\partial t} \right|_A = \sum_{\mu=1}^{N_T} \left[\frac{1}{2}\omega_{21}(2\sigma_{\mu}^{-}\rho\sigma_{\mu}^{+} - \sigma_{\mu}^{+}\sigma_{\mu}^{-}\rho - \rho\sigma_{\mu}^{+}\sigma_{\mu}^{-}) + \frac{1}{2}\omega_{12}(2\sigma_{\mu}^{+}\rho\sigma_{\mu}^{-} - \sigma_{\mu}^{-}\sigma_{\mu}^{+}\rho - \rho\sigma_{\mu}^{-}\sigma_{\mu}^{+}) \right.$$

$$+ \frac{1}{2}\omega_{10}(2\chi_{\mu}^{-}\rho\chi_{\mu}^{+} - \chi_{\mu}^{+}\chi_{\mu}^{-}\rho - \rho\chi_{\mu}^{+}\chi_{\mu}^{-}) + \frac{1}{2}\omega_{01}(2\chi_{\mu}^{+}\rho\chi_{\mu}^{-} - \chi_{\mu}^{-}\chi_{\mu}^{+}\rho - \rho\chi_{\mu}^{-}\chi_{\mu}^{+})$$

$$\left. + \frac{1}{2}\omega_{20}(2\phi_{\mu}^{-}\rho\phi_{\mu}^{+} - \phi_{\mu}^{+}\phi_{\mu}^{-}\rho - \rho\phi_{\mu}^{+}\phi_{\mu}^{-}) + \frac{1}{2}\omega_{02}(2\phi_{\mu}^{+}\rho\phi_{\mu}^{-} - \phi_{\mu}^{-}\phi_{\mu}^{+}\rho - \rho\phi_{\mu}^{-}\phi_{\mu}^{+}) \right]. \quad (2.11)$$

In writing (2.11) we have assumed only terms representing level transitions are to be included in the atomic damping, that is, all terms proportional to ω_{ii} in (2.5) are zero.

III. THE CHARACTERISTIC FUNCTION AND EQUATION

Following the procedure in Ref. 1, we introduce the characteristic function χ as

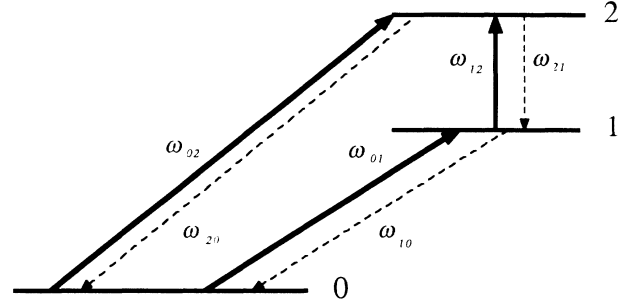


FIG. 2. Diagram showing the master equation level transitions.

$$I_{\mu}^1 = \begin{pmatrix} 1 & 0 & 0 \\ 0 & 0 & 0 \\ 0 & 0 & 0 \end{pmatrix}, \quad I_{\mu}^2 = \begin{pmatrix} 0 & 0 & 0 \\ 0 & 1 & 0 \\ 0 & 0 & 1 \end{pmatrix}. \quad (2.9)$$

The following algebra may then be derived: (i)

$$\chi_{\mu}^{+}I_{\mu}^1 = \chi_{\mu}^{+} = I_{\mu}^2\chi_{\mu}^{+}, \quad \chi_{\mu}^{-}I_{\mu}^2 = \chi_{\mu}^{-} = I_{\mu}^1\chi_{\mu}^{-},$$

$$\chi_{\mu}^{-}\sigma_{\mu,z} = -\frac{1}{2}\chi_{\mu}^{-}, \quad \sigma_{\mu,z}\chi_{\mu}^{+} = -\frac{1}{2}\chi_{\mu}^{+}, \quad \chi_{\mu}^{-}\sigma_{\mu}^{-} = \phi_{\mu}^{-},$$

$$\sigma_{\mu}^{+}\chi_{\mu}^{+} = \phi_{\mu}^{+},$$

(ii)

$$\phi_{\mu}^{+}I_{\mu}^1 = \phi_{\mu}^{+} = I_{\mu}^2\phi_{\mu}^{+}, \quad \phi_{\mu}^{-}I_{\mu}^2 = \phi_{\mu}^{-} = I_{\mu}^1\phi_{\mu}^{-},$$

$$\phi_{\mu}^{-}\sigma_{\mu,z} = \frac{1}{2}\phi_{\mu}^{-}, \quad \sigma_{\mu,z}\phi_{\mu}^{+} = \frac{1}{2}\phi_{\mu}^{+}, \quad \phi_{\mu}^{-}\sigma_{\mu}^{+} = \chi_{\mu}^{-},$$

$$\sigma_{\mu}^{-}\phi_{\mu}^{+} = \chi_{\mu}^{+},$$

(iii)

$$\chi_{\mu}^{-}\chi_{\mu}^{+} = I_{\mu}^1 = \phi_{\mu}^{-}\phi_{\mu}^{+}, \quad \chi_{\mu}^{+}\chi_{\mu}^{-} = \frac{1}{2}I_{\mu}^2 - \sigma_{\mu,z},$$

$$\phi_{\mu}^{+}\phi_{\mu}^{-} = \frac{1}{2}I_{\mu}^2 + \sigma_{\mu,z}, \quad \chi_{\mu}^{+}\phi_{\mu}^{-} = \sigma_{\mu}^{-}, \quad \phi_{\mu}^{+}\chi_{\mu}^{-} = \sigma_{\mu}^{+}.$$

All other matrix products are zero. So substituting these operators into (2.3), the terms in the master equation are now written as

$$\chi = \text{Tr}(O\rho), \quad (3.1)$$

where $O = O^A O^F$ or $O = Q^{A,\mu} O^{A,\mu}$,

$$O^F = \exp(i\beta^+ a^{\dagger}) \exp(i\beta a), \quad (3.2)$$

$$O^A = \prod_{\mu=1}^{N_T} O^{A,\mu}, \quad (3.3)$$

$$Q^{A,\mu} = O^F \prod_{\substack{i=1 \\ i \neq \mu}}^{N_T} O^{A,i}. \quad (3.4)$$

The kernel $O^{A,\mu}$ is defined to be a linear combination of the operators representing the atoms, as in the two-level situation. However, to include the effect of the third level and obtain a closed set of variables, we now define

$$O^{A,\mu} = b_1 I_\mu^1 + b I_\mu^2 + \mathbf{c} \cdot \boldsymbol{\sigma}_\mu. \quad (3.5)$$

The differential equation for the characteristic function is

given by

$$\frac{\partial \chi}{\partial t} = \text{Tr} \left[O \frac{\partial \rho}{\partial t} \right]. \quad (3.6)$$

This equation will contain all the terms from the two-level model, but in addition there will be contributions related to the ground level. The method is identical to that of the two-level atom model, however now using the third level algebra and gives terms like

$$\begin{aligned} \text{Tr}(O \omega_{10} \chi_\mu^- \rho \chi_\mu^+) &= \omega_{10} \text{Tr} \left[\sum_{\mu=1}^{N_T} Q^{A,\mu} (b_1 I_\mu^1 + b I_\mu^2 + \mathbf{c} \cdot \boldsymbol{\sigma}_\mu) \chi_\mu^- \rho \chi_\mu^+ \right] \\ &= \omega_{10} \text{Tr} \left[\sum_{\mu=1}^{N_T} Q^{A,\mu} (b_1 \chi_\mu^+ I_\mu^1 \chi_\mu^- + b \chi_\mu^+ I_\mu^2 \chi_\mu^- + c \chi_\mu^+ \sigma_{\mu,z} \chi_\mu^- + c^+ \chi_\mu^+ \sigma_\mu^+ \sigma_\mu^- + c^- \chi_\mu^+ \sigma_\mu^- \chi_\mu^-) \rho \right] \\ &= \omega_{10} \text{Tr} \left[\sum_{\mu=1}^{N_T} Q^{A,\mu} b_1 \left(\frac{1}{2} I_\mu^2 - \sigma_{\mu,z} \right) \rho \right] \\ &= \omega_{10} \text{Tr} \left[\sum_{\mu=1}^{N_T} Q^{A,\mu} b_1 \left[\frac{1}{2} \frac{\partial}{\partial b} - \frac{\partial}{\partial c} \right] O^{A,\mu} \rho \right] \\ &= \omega_{10} b_1 \left[\frac{1}{2} \frac{\partial}{\partial b} - \frac{\partial}{\partial c} \right] \chi. \end{aligned} \quad (3.7)$$

Combining all the various contributions to (3.6) we finally obtain

$$\begin{aligned} \frac{\partial \chi}{\partial t} &= \left\{ \kappa \left[-i\beta \frac{\partial}{\partial i\beta} - i\beta^+ \frac{\partial}{\partial i\beta^+} + 2ni\beta^+ i\beta + (i\beta)^2 m + (i\beta^+)^2 m^* \right] - \frac{1}{2}(\omega_{12} + \omega_{21}) \left[c^+ \frac{\partial}{\partial c^+} + c^- \frac{\partial}{\partial c^-} + 2c \frac{\partial}{\partial c} \right] \right. \\ &\quad + \frac{1}{2}(\omega_{12} - \omega_{21}) c \frac{\partial}{\partial b} + \frac{1}{2}(\omega_{10} + \omega_{20}) \left[(b_1 - b) \frac{\partial}{\partial b} - c \frac{\partial}{\partial c} - c^+ \frac{\partial}{\partial c^+} - c^- \frac{\partial}{\partial c^-} \right] - \frac{1}{2}(\omega_{01} - \omega_{02}) c \frac{\partial}{\partial b_1} \\ &\quad - (\omega_{10} - \omega_{20}) \left[(b_1 - b) \frac{\partial}{\partial c} - \frac{1}{4} c \frac{\partial}{\partial b} \right] - (\omega_{01} + \omega_{02}) (b_1 - b) \frac{\partial}{\partial b_1} \\ &\quad + g \left[-c \frac{\partial^2}{\partial c^+ \partial i\beta} + 2c^- \frac{\partial^2}{\partial c \partial i\beta} + i\beta \left[(b - \frac{1}{2}c) \frac{\partial}{\partial c^-} + c^+ \left[\frac{1}{2} \frac{\partial}{\partial b} + \frac{\partial}{\partial c} \right] \right] - c \frac{\partial^2}{\partial c^- \partial i\beta^+} + 2c^+ \frac{\partial^2}{\partial c \partial i\beta^+} \right. \\ &\quad \left. + i\beta^+ \left[(b - \frac{1}{2}c) \frac{\partial}{\partial c^+} + c^- \left[\frac{1}{2} \frac{\partial}{\partial b} + \frac{\partial}{\partial c} \right] \right] \right] \chi. \end{aligned} \quad (3.9)$$

IV. TRANSFORMATION TO THE FOKKER-PLANCK EQUATION

To be consistent with Ref. 1 we first make the change of variables

$$b \rightarrow 1 + b', \quad b_1 \rightarrow 1 + b'_1. \quad (4.1)$$

We then use a generalized P distribution to convert the characteristic function equation into an equation involving classical variables in phase space. This is achieved by the particular choice of a positive- P function as

$$\chi(\mathbf{y}) = \int \cdots \int d\mathbf{x} \exp[i(\beta^+, \beta, c^+, \frac{1}{2}c, c^-, b', b'_1) \cdot \mathbf{x}] P(\mathbf{x}), \quad (4.2)$$

where $\mathbf{x} = (\alpha^+, \alpha, \nu^+, D, \nu, B, B_1)^T$ and $\mathbf{y} = (\beta^+, \beta, c^+, c, c^-, b', b'_1)^T$. As explicitly indicated, variables are not complex conjugates of the corresponding variables with the superscript $+$, but instead define the P function in an extended 14-dimensional phase-space. As was shown in Ref. 4 this positive P function explicitly has positive semidefinite diffusion. Now under the assumption that the surface terms vanish as the phase-space integration sphere tends towards infinity, the following Fokker-Planck equation is derived:

$$\begin{aligned}
\frac{\partial}{\partial t} P(\mathbf{x}) = & \left\{ \kappa \left[\frac{\partial}{\partial \alpha} \alpha + \frac{\partial}{\partial \alpha^+} \alpha^+ + \frac{\partial^2}{\partial \alpha \partial \alpha^+} 2n + \frac{\partial^2}{\partial \alpha^2} m + \frac{\partial^2}{\partial \alpha^+{}^2} m^* \right] + \frac{1}{2}(\omega_{12} + \omega_{21}) \left[\frac{\partial}{\partial v} v + \frac{\partial}{\partial v^+} v^+ + 2 \frac{\partial}{\partial D} D \right] \right. \\
& - (\omega_{12} - \omega_{21}) \frac{\partial}{\partial B} B + \frac{1}{2}(\omega_{10} + \omega_{20}) \left[\frac{\partial}{\partial v} v + \frac{\partial}{\partial v^+} v^+ + \frac{\partial}{\partial D} D + \left[\frac{\partial}{\partial B} - \frac{\partial}{\partial B_1} \right] B \right] + (\omega_{01} - \omega_{02}) \frac{\partial}{\partial D} B_1 \\
& + \frac{1}{2}(\omega_{10} - \omega_{20}) \left[\left[\frac{\partial}{\partial B_1} - \frac{\partial}{\partial B} \right] D - \frac{\partial}{\partial B} B \right] + (\omega_{01} + \omega_{02}) \left[\frac{\partial}{\partial B_1} - \frac{\partial}{\partial B} \right] B_1 \\
& + g \left[2 \frac{\partial}{\partial D} (\alpha v^+ + \alpha^+ v) - \frac{\partial}{\partial v} \alpha D - \frac{\partial}{\partial v^+} \alpha^+ D - \frac{\partial}{\partial \alpha} v - \frac{\partial}{\partial \alpha^+} v^+ + \left[\frac{\partial^2}{\partial v \partial \alpha^+} + \frac{\partial^2}{\partial v^+ \partial \alpha} \right] \frac{1}{2}(B + D) \right. \\
& \left. + \left[\frac{\partial}{\partial B} - \frac{\partial}{\partial D} \right] \left[\frac{\partial}{\partial \alpha} v + \frac{\partial}{\partial \alpha^+} v^+ \right] \right\} P(\mathbf{x}) . \tag{4.3}
\end{aligned}$$

The first thing to notice is that the second-order noise terms are independent of the terms involving transitions to and from the ground level. This means that by introducing a ground level in addition to the lasing levels, we are not further complicating the quantum noise, but just affecting the deterministic properties of the laser. The corresponding stochastic differential equations are

$$\begin{aligned}
\dot{\alpha} &= -\kappa \alpha + g v + \Gamma_{\alpha} , \\
\dot{\alpha}^+ &= -\kappa \alpha^+ + g v^+ + \Gamma_{\alpha^+} , \\
\dot{v} &= -\left[\frac{1}{2}(\omega_{12} + \omega_{21}) + \frac{1}{2}(\omega_{10} + \omega_{20}) \right] v + g \alpha D + \Gamma_v , \\
\dot{v}^+ &= -\left[\frac{1}{2}(\omega_{12} + \omega_{21}) + \frac{1}{2}(\omega_{10} + \omega_{20}) \right] v^+ + g \alpha^+ D + \Gamma_{v^+} , \\
\dot{D} &= -\left[\omega_{12} + \omega_{21} + \frac{1}{2}(\omega_{10} + \omega_{20}) \right] D + (\omega_{02} - \omega_{01}) B_1 - 2g(\alpha^+ v + \alpha v^+) + \left[\omega_{12} - \omega_{21} + \frac{1}{2}(\omega_{10} - \omega_{20}) \right] B + \Gamma_D , \\
\dot{B} &= -\frac{1}{2}(\omega_{10} + \omega_{20}) B + \frac{1}{2}(\omega_{10} - \omega_{20}) D + (\omega_{01} + \omega_{02}) B_1 + \Gamma_B , \\
\dot{B}_1 &= \frac{1}{2}(\omega_{10} + \omega_{20}) B - \frac{1}{2}(\omega_{10} - \omega_{20}) D - (\omega_{01} + \omega_{02}) B_1 ,
\end{aligned} \tag{4.4}$$

where $\langle \Gamma_i(t) \Gamma_j(t') \rangle = d_{ij} \delta(t - t')$, and the diffusion matrix d is

$$\mathbf{d} = \begin{pmatrix} 2\kappa m & 2\kappa n & 0 & \frac{1}{2}g(B + D) & -g v & g v & 0 \\ 2\kappa n & 2\kappa m^* & \frac{1}{2}g(B + D) & 0 & -g v^+ & g v^+ & 0 \\ 0 & \frac{1}{2}g(B + D) & 0 & 0 & 0 & 0 & 0 \\ \frac{1}{2}g(B + D) & 0 & 0 & 0 & 0 & 0 & 0 \\ -g v & -g v^+ & 0 & 0 & 0 & 0 & 0 \\ g v & g v^+ & 0 & 0 & 0 & 0 & 0 \\ 0 & 0 & 0 & 0 & 0 & 0 & 0 \end{pmatrix} . \tag{4.5}$$

In our previous paper,¹ the variable B which had all moments equal to the moments of the number of lasing atoms (fixed), was unstable because of the effect of the quantum noise. However, in (4.4), this variable now has stabilizing deterministic terms. These terms are all proportional to transition rates to and from the ground level, indicating that the ground level is fundamental to the stability of the laser operation for this model. Of course, there is a price in that the number of lasing atoms is no longer a constant but fluctuates around some average number of atoms. Nevertheless, in many respects this is a more realistic description of the number of lasing atoms in a true laser.

If we now define the variable $B_2 = B + B_1$, then it will have the stochastic equation

$$\dot{B}_2 = \dot{B} + \dot{B}_1 = \Gamma_B . \tag{4.6}$$

The moments of B_2 will all be equal to those of N_T —the total number of atoms in the three-level model—which is fixed. However, the equation for B_2 has been made unstable by a noise term proportional to the coupling constant g , which has no apparent physical interpretation. This can only be eliminated by adding a fourth level, in which case B_2 is stabilized at the expense of an instability in B_3 , the variable with moments equaling that of the total number of four-level atoms. By adding further levels this instability may be shifted further from the lasing levels, but the instability cannot be eliminated. It seems most likely that this instability is simply an artifact of the way our formalism treats interactions between atoms and

light fields. In the next section we introduce an assumption on the character of the ground level which allows us to remove this instability and obtain useful results.

V. MODELS FOR THE LASER

A. Laser model 1

In the traditional two-level laser model we require (from Fig. 2)

$$\omega_{12}=2\gamma, \quad \omega_{21}=0. \quad (5.1)$$

(Strictly speaking, ω_{21} cannot be zero—rather, we consider the case when it is small compared to other terms.) Thus the bath pumps so that only transitions from level 1 to level 2 are allowed. Incorporating the third level, we stabilize the B equation by allowing transitions connecting the ground level and both the upper lasing levels, i.e.,

$$\omega_{20}=a=\omega_{10}, \quad \omega_{02}=Xa=\omega_{01}. \quad (5.2)$$

The parameter X relates the upward transition rates to those of the downward transitions. At this stage we have assumed equal transition rates between each of the upper levels and the ground level, as this is all that is required for stability reasons. The stochastic differential equations (4.4) then become

$$\begin{aligned} \dot{\alpha} &= -\kappa\alpha + g\nu + \Gamma_\alpha, \\ \dot{\nu} &= -(\gamma + a)\nu + g\alpha D + \Gamma_\nu, \\ \dot{D} &= -(2\gamma + a)D + 2\gamma B - 2g(\alpha^+\nu + \alpha\nu^+) + \Gamma_D, \\ \dot{B} &= -aB + 2XaB_1 + \Gamma_B, \\ \dot{B}_1 &= aB - 2XaB_1. \end{aligned} \quad (5.3)$$

Here and in what follows, we will not explicitly write out the equations for α^+ and ν^+ —they may be simply found by treating them as pseudo-complex-conjugate equations to those for α and ν . Now to remove the instability we employ the same approximation as Gordon² by considering nearly all the atoms to be in the ground state and that N_T , the total number of atoms, is very large. Thus the ground level acts as extra bath to the lasing levels and since in the initial condition $B_1 \approx N_T$ and \dot{B}_1/B_1 is very small, we can drop the equation for B_1 and treat B_1 as the constant N_T . This, of course, requires X to be very small. So defining $N = 2XB_1 = 2XN_T$ to be the average number of atoms in the lasing levels, we obtain

$$\begin{aligned} \dot{\alpha} &= -\kappa\alpha + g\nu + \Gamma_\alpha, \\ \dot{\nu} &= -(\gamma + a)\nu + g\alpha D + \Gamma_\nu, \\ \dot{D} &= -(2\gamma + a)D + 2\gamma B - 2g(\alpha^+\nu + \alpha\nu^+) + \Gamma_D, \\ \dot{B} &= -a(B - N) + \Gamma_B. \end{aligned} \quad (5.4)$$

In the limit of $a \rightarrow 0$ these equations are identical to those obtained using our two-level laser model. Performing a semiclassical analysis

$$B = N, \quad \nu = \frac{g\alpha D}{\gamma + a}, \quad D = \frac{N}{1 + \frac{a}{2\gamma} + \frac{2g^2\alpha\alpha^+}{\gamma(\gamma + a)}}. \quad (5.5)$$

The introduction of a affects and reduces the steady-state inversion, so we therefore require a to be small. The total model we wish to consider, then, is where the inversion is determined by the discrepancy between ω_{12} and ω_{21} and the connection with the ground level acts as a slow mechanism to ensure that the total number of lasing atoms fluctuates around the average N .

B. Laser model 2

The ground level allows greater freedom in the method of pumping the upper lasing level. Perhaps a more physical method of creating an inversion is to follow the model described by Loudon⁹ and set

$$\omega_{02}=Xa, \quad \omega_{01}=0, \quad \omega_{20}=a=\omega_{10}, \quad \omega_{12}=\gamma=\omega_{21}, \quad (5.6)$$

where a pumping mechanism is used to excite ground-level atoms into the upper lasing level, but not into the lower lasing level. The stochastic differential equations are then

$$\begin{aligned} \dot{\alpha} &= -\kappa\alpha + g\nu + \Gamma_\alpha, \\ \dot{\nu} &= -(\gamma + a)\nu + g\alpha D + \Gamma_\nu, \\ \dot{D} &= -(2\gamma + a)D + XaB_1 - 2g(\alpha^+\nu + \alpha\nu^+) + \Gamma_D, \\ \dot{B} &= -aB + XaB_1 + \Gamma_B, \\ \dot{B}_1 &= aB - XaB_1. \end{aligned} \quad (5.7)$$

We again consider the ground level to be a reservoir containing an effectively infinite number of atoms and thus drop the B_1 equation, setting $B_1 \approx N_T$. If we now define $N = XN_T$ as the average number of lasing atoms, we obtain the system

$$\begin{aligned} \dot{\alpha} &= -\kappa\alpha + g\nu + \Gamma_\alpha, \\ \dot{\nu} &= -(\gamma + a)\nu + g\alpha D + \Gamma_\nu, \\ \dot{D} &= -(2\gamma + a)D + aN - 2g(\alpha^+\nu + \alpha\nu^+) + \Gamma_D, \\ \dot{B} &= -a(B - N) + \Gamma_B. \end{aligned} \quad (5.8)$$

A semiclassical analysis gives

$$B = N, \quad \nu = \frac{g\alpha D}{\gamma + a}, \quad D = \frac{N}{1 + \frac{2\gamma}{a} + \frac{4g^2\alpha\alpha^+}{a(\gamma + a)}}. \quad (5.9)$$

We therefore require the ratio γ/a to be small in order to maintain a significant population inversion. The parameter a can now be set to be quite large, so that the variable B representing the number of lasing atoms is stabilized more quickly about the average number of lasing atoms. Furthermore, the stability properties of the equation for the inversion D are now improved as the inversion driving term from model 1 of $2\gamma B$, which fluctuated around N , is now replaced with a term simply proportional to N .

C. Laser model 3

The final model that we will consider is one where the inversion is created by both of the mechanisms in models 1 and 2, i.e.,

$$\omega_{12}=2\gamma, \quad \omega_{02}=Xa, \quad \omega_{01}=0=\omega_{21}, \quad \omega_{10}=\omega_{20}=\alpha. \quad (5.10)$$

Following the same procedure as above, we drop the B_1 equation and define $N=XN_T$, to give the system

$$\begin{aligned} \dot{\alpha} &= -\kappa\alpha + g\nu + \Gamma_\alpha, \\ \dot{\nu} &= -(\gamma+a)\nu + g\alpha D + \Gamma_\nu, \\ \dot{D} &= -(2\gamma+a)D + aN + 2\gamma B - 2g(\alpha^+\nu + \alpha\nu^+) + \Gamma_D, \\ \dot{B} &= -a(B-N) + \Gamma_B. \end{aligned} \quad (5.11)$$

The semiclassical inversion is then

$$D = \frac{N}{1 + \frac{4g^2\alpha\alpha^+}{(2\gamma+a)(\gamma+a)}}. \quad (5.12)$$

This model now allows γ and a to become arbitrarily large without reducing the steady-state inversion. A large value of a could then improve the stability, but there will still be fluctuations due to the inversion driving term $2\gamma B$, a term which is not present in model 2.

D. Optical bistability model

To analyze optical bistability for a three-level system we include the standard cavity driving term in the Hamiltonian model

$$H_4 = i\hbar(a^\dagger \epsilon e^{-i\omega t} - a \epsilon^* e^{i\omega t}). \quad (5.13)$$

This then changes the stochastic equation for the cavity variable to

$$\dot{\alpha} = \epsilon - \kappa\alpha + g\nu + \Gamma_\alpha. \quad (5.14)$$

We now require there to be a negative inversion to get bistability, that is, we organize the atomic transitions so that the majority of the non-ground-level atoms are in the lower lasing level. The most general way to write down the transitions is then

$$\begin{aligned} \omega_{12} - \omega_{21} &= 2X_0\gamma, \quad \omega_{12} + \omega_{21} = 2\gamma, \\ \omega_{02} - \omega_{01} &= X_0Xa, \quad \omega_{01} + \omega_{02} = Xa, \quad \omega_{20} = a = \omega_{10}. \end{aligned} \quad (5.15)$$

The choice $X_0=1$ corresponds to a laser configuration,

whereas $X_0=-1$ is suitable for either analyzing optical bistability or the Jaynes-Cumming model. After assuming the ground level acts as an extra bath we obtain the system

$$\begin{aligned} \dot{\alpha} &= \epsilon - \kappa\alpha + g\nu + \Gamma_\alpha, \\ \dot{\nu} &= -(\gamma+a)\nu + g\alpha D + \Gamma_\nu, \\ \dot{D} &= -(2\gamma+a)D + X_0(aN + 2\gamma B) - 2g(\alpha^+\nu + \alpha\nu^+) + \Gamma_D, \\ \dot{B} &= -a(B-N) + \Gamma_B. \end{aligned} \quad (5.16)$$

VI. SCALING THE LASER EQUATIONS

We would expect the macroscopic atomic variables to be proportional to the number of lasing atoms N and to explicitly show this we make the scaling

$$\nu, \nu^+, D, B \rightarrow \tilde{\nu}N, \tilde{\nu}^+N, \tilde{D}N, \tilde{B}N. \quad (6.1)$$

In addition, it is reasonable to expect the coupling constant g to scale with the number of lasing atoms as (this is the standard assumption made by Haken¹⁰)

$$g \rightarrow \tilde{g}N^{-1/2}. \quad (6.2)$$

Now selecting model 2 from Sec. V as the most physically reasonable three-level atom laser or optical bistability model, then we scale the cavity variables as

$$\alpha \rightarrow \frac{\bar{\alpha}N^{1/2}}{s}, \quad \alpha^+ \rightarrow \frac{\bar{\alpha}^+N^{1/2}}{s}, \quad (6.3)$$

where $s = \tilde{g}/a$, is the ratio of the scaled coupling constant to the pumping rate. Finally, we also scale the time in terms of the atomic pumping rate, to give the scaled time unit

$$\tau = at. \quad (6.4)$$

The scaling transformations (6.1)–(6.4) may then be performed either from the Fokker-Planck equation or the stochastic equations and results in the scaled system

$$\begin{aligned} \dot{\bar{\alpha}} &= \eta(Z - \bar{\alpha} + C\tilde{\nu}) + \Gamma_{\bar{\alpha}}, \\ \dot{\tilde{\nu}} &= -(1+\gamma')\tilde{\nu} + \bar{\alpha}\tilde{D} + \Gamma_{\tilde{\nu}}, \\ \dot{\tilde{D}} &= -(1+2\gamma')\tilde{D} + X_0 - 2(\bar{\alpha}^+\tilde{\nu} + \bar{\alpha}\tilde{\nu}^+) + \Gamma_{\tilde{D}}, \\ \dot{\tilde{B}} &= -(\tilde{B}-1) + \Gamma_{\tilde{B}}, \end{aligned} \quad (6.5)$$

where the diffusion matrix satisfying $\langle \Gamma_{\bar{x}}(\tau)\Gamma_{\bar{y}}(\tau') \rangle = d_{\bar{x}\bar{y}}\delta(\tau-\tau')$ is given by

$$d = \frac{s^2}{N} \begin{pmatrix} 2\eta m & 2\eta n & 0 & \frac{1}{2}(\tilde{B} + \tilde{D}) & -\tilde{\nu} & \tilde{\nu} \\ 2\eta n & 2\eta m^* & \frac{1}{2}(\tilde{B} + \tilde{D}) & 0 & -\tilde{\nu}^+ & \tilde{\nu}^+ \\ 0 & \frac{1}{2}(\tilde{B} + \tilde{D}) & 0 & 0 & 0 & 0 \\ \frac{1}{2}(\tilde{B} + \tilde{D}) & 0 & 0 & 0 & 0 & 0 \\ -\tilde{\nu} & -\tilde{\nu}^+ & 0 & 0 & 0 & 0 \\ \tilde{\nu} & \tilde{\nu}^+ & 0 & 0 & 0 & 0 \end{pmatrix}, \quad (6.6)$$

$\eta = \kappa/a$ gives the ratio of cavity damping to atomic pumping, $\gamma' = \gamma/a$ gives the ratio of lasing level transitions to atomic pumping, $C = \bar{g}s/\kappa = s^2/\eta$ is the cooperativity parameter, and $n_s = \frac{1}{4}(a/g)^2 = N/4s^2$ is the saturation photon number.

In this scaling, since $d_{ij} \propto 1/n_s$, it clearly shows that the semiclassical predictions will be valid in situations with large saturation photon numbers, because of either a large number of atoms (the traditional laser scaling), or a small value of the parameter s .

Finally, in optical bistability situations, the nonzero scaled cavity driving field is given by

$$Z = \frac{\epsilon s}{N^{1/2}\kappa}, \quad (6.7)$$

where ϵ is as defined in (5.13). If C is finite, small s implies a good cavity, since this necessarily implies that η , the ratio of cavity damping to atomic pumping, is small.

VII. SOLUTION BY ADIABATIC ELIMINATION OF THE ATOMS

We now consider an approximate solution of the system of equations (6.5) which is valid in the adiabatic elimination limit $\eta \ll 1$, that is, where the ratio of the cavity damping to the atomic pumping rate is small. This is the usual regime for laser operation and following the standard analysis we assume that in the time scale of interest

$$\dot{\bar{v}} = 0, \quad \dot{\bar{D}} = 0, \quad \dot{\bar{B}} = 0. \quad (7.1)$$

The atomic variables then assume the stationary values

$$\bar{B} = 1 + \Gamma_{\bar{B}}, \quad (7.2)$$

$$\bar{D} = X_0\Pi - \frac{2\Pi}{1+\gamma'}(\bar{\alpha}^+ \Gamma_{\bar{v}} + \alpha \Gamma_{\bar{v}^+}) + \Pi\Gamma_{\bar{D}}, \quad (7.3)$$

$$\bar{v} = \frac{\bar{\alpha} X_0\Pi}{1+\gamma'} + \frac{\Gamma_{\bar{v}}}{1+\gamma'} \left[1 - \frac{2\bar{\alpha} \bar{\alpha}^-}{1+\gamma'} \right] + \frac{\bar{\alpha} \Pi\Gamma_{\bar{D}}}{1+\gamma'} - \frac{2\bar{\alpha}^2 \Pi\Gamma_{\bar{v}^+}}{(1+\gamma')^2}, \quad (7.4)$$

where

$$\Pi = \frac{1}{1+2\gamma' + \frac{4\bar{\alpha} \bar{\alpha}^+}{1+\gamma'}}.$$

The cavity field equations are then

$$\dot{\bar{\alpha}} = \eta \left[Z - \bar{\alpha} + \frac{C\bar{\alpha}X_0\Pi}{1+\gamma'} \right] + F_{\bar{\alpha}}, \quad (7.5)$$

$$\dot{\bar{\alpha}}^+ = \eta \left[Z^* - \bar{\alpha}^+ + \frac{C\bar{\alpha}^+X_0\Pi}{1+\gamma'} \right] + F_{\bar{\alpha}^+},$$

with the stochastic terms

$$F_{\bar{\alpha}} = \Gamma_{\bar{\alpha}} + \frac{s^2}{1+\gamma'} \left[\Gamma_{\bar{v}} \left[1 - \frac{2\bar{\alpha} \bar{\alpha}^+ \Pi}{1+\gamma'} \right] + \bar{\alpha} \Pi\Gamma_{\bar{D}} - \frac{2\bar{\alpha}^2 \Pi\Gamma_{\bar{v}^+}}{1+\gamma'} \right], \quad (7.6)$$

$$F_{\bar{\alpha}^+} = \Gamma_{\bar{\alpha}^+} + \frac{s^2}{1+\gamma'} \left[\Gamma_{\bar{v}^+} \left[1 - \frac{2\bar{\alpha} \bar{\alpha}^+ \Pi}{1+\gamma'} \right] + \bar{\alpha}^+ \Pi\Gamma_{\bar{D}} - \frac{2\bar{\alpha}^+ \Pi\Gamma_{\bar{v}}}{1+\gamma'} \right].$$

We now work out the leading noise terms for the $\bar{\alpha}, \bar{\alpha}^+$ cavity system. This requires the first order approximation for the atomic variables from Eqs. (7.2)–(7.4)

$$\bar{B} = 1, \quad \bar{D} = X_0\Pi, \quad \bar{v} = \frac{\bar{\alpha}X_0\Pi}{1+\gamma'}, \quad (7.7)$$

which is justified for large saturation photon numbers where the diffusion terms are small. Hence we calculate

$$\langle F_{\bar{\alpha}} F_{\bar{\alpha}^+} \rangle = \langle \Gamma_{\bar{\alpha}} \Gamma_{\bar{\alpha}^+} \rangle + \frac{s^2}{1+\gamma'} \left[(\langle \Gamma_{\bar{\alpha}} \Gamma_{\bar{v}^+} \rangle + \langle \Gamma_{\bar{\alpha}^+} \Gamma_{\bar{v}} \rangle) \left[1 - \frac{2\bar{\alpha} \bar{\alpha}^+ \Pi}{1+\gamma'} \right] + \bar{\alpha}^+ \Pi \langle \Gamma_{\bar{\alpha}} \Gamma_{\bar{D}} \rangle + \bar{\alpha} \Pi \langle \Gamma_{\bar{\alpha}^+} \Gamma_{\bar{D}} \rangle \right]. \quad (7.8)$$

Now using the diffusion coefficients in (6.6) and replacing the atomic variables using (7.7), we finally obtain

$$\langle F_{\bar{\alpha}} F_{\bar{\alpha}^+} \rangle = \frac{s^2}{N} \left[2\eta n + \frac{s^2}{1+\gamma'} \left[(1+X_0\Pi) \left[1 - \frac{2\bar{\alpha} \bar{\alpha}^+ \Pi}{1+\gamma'} \right] - \frac{2X_0 \bar{\alpha} \bar{\alpha}^+ \Pi^2}{1+\gamma'} \right] \right]. \quad (7.9)$$

In a similar fashion the other noise terms can be evaluated as

$$\langle F_{\bar{\alpha}} F_{\bar{\alpha}} \rangle = \frac{s^2}{N} \left[2\eta m - \frac{s^2 \bar{\alpha}^2}{(1+\gamma')^2} [2X_0\Pi^2 + 2\Pi(1+X_0\Pi)] \right], \quad (7.10)$$

$$\langle F_{\bar{\alpha}^+} F_{\bar{\alpha}^+} \rangle = \frac{s^2}{N} \left[2\eta m^* - \frac{s^2 \bar{\alpha}^+{}^2}{(1+\gamma')^2} [2X_0\Pi^2 + 2\Pi(1+X_0\Pi)] \right]. \quad (7.11)$$

These expressions are completely general, requiring only that η and $1/n_s$ be small and hence lead to a Fokker-

Planck description of the cavity field for the laser and optical bistability without any elimination of higher-order derivative terms. The Fokker-Planck equation obtained, is, of course, difficult to solve exactly, although a linearized solution may be found using standard techniques¹¹ for optical bistability. However, by considering more carefully the expressions (7.9)–(7.11) for large and small intensity situations, we are able to isolate the dominant noise terms and thus simplify the corresponding Fokker-Planck equation.

A. Small intensity solution (with $\gamma'=0$)

Where the cavity intensity is small we may expand Π as

$$\Pi = 1 - 4\bar{\alpha}\bar{\alpha}^+ + 32\bar{\alpha}^2\bar{\alpha}^{+2} - \dots, \quad (7.12)$$

to obtain

$$\begin{aligned} \langle F_{\bar{\alpha}} F_{\bar{\alpha}^+} \rangle &= \frac{s^2}{N} (2\eta n + s^2 \{ (1 + X_0) - \bar{\alpha}\bar{\alpha}^+ [6X_0 + 2(1 + X_0)] \}), \end{aligned} \quad (7.13)$$

$$\langle F_{\bar{\alpha}} F_{\bar{\alpha}} \rangle = \frac{s^2}{N} \{ 2\eta m - s^2 \bar{\alpha}^2 [2X_0 + 2(1 + X_0)] \}. \quad (7.14)$$

For a laser configuration we set $X_0=1$ and to zeroth order in the intensity the leading noise terms are

$$\langle F_{\bar{\alpha}} F_{\bar{\alpha}^+} \rangle = \frac{s^2}{N} (2\eta n + 2s^2), \quad \langle F_{\bar{\alpha}} F_{\bar{\alpha}} \rangle = \frac{s^2}{N} 2\eta m. \quad (7.15)$$

These terms are exactly equivalent to those obtained for the two-level laser model in our previous paper. With the choice $m, m^*=0$ the simplified Fokker-Planck equation (FPE) obtained from (7.15) has a potential solution describing the usual laser operation.¹²

If we now set $X_0=-1$, then the spontaneous-emission term which dominated in (7.15) vanishes and to first order in intensity we obtain

$$\begin{aligned} \langle F_{\bar{\alpha}} F_{\bar{\alpha}^+} \rangle &= \frac{s^2}{N} (2\eta n + 6\bar{\alpha}\bar{\alpha}^+ + s^2), \\ \langle F_{\bar{\alpha}} F_{\bar{\alpha}} \rangle &= \frac{s^2}{N} (2\eta m + 2\bar{\alpha}^2 s^2). \end{aligned} \quad (7.16)$$

We now have a simplified FPE describing optical bistability, without the third-order terms present in Ref. 1. In general, this Fokker-Planck equation has no potential solution, but in the particular case $Z=0$ (i.e., zero driving field) where we consider Jaynes-Cummings-type problems, a potential solution is found and stationary photon statistics may be derived.

B. Large intensity solution (with $\gamma'=0$)

In situations where the intensity is large, we may make the alternate expansion

$$\Pi = \frac{1}{4\bar{\alpha}\bar{\alpha}^+} \left[1 - \frac{1}{4\bar{\alpha}\bar{\alpha}^+} + \dots \right]. \quad (7.17)$$

The leading noise terms in both the laser and optical bistability configurations to zeroth order in the inverse intensity are now found to be

$$\begin{aligned} \langle F_{\bar{\alpha}} F_{\bar{\alpha}^+} \rangle &= \frac{s^2}{N} (2\eta n + \frac{1}{2}s^2), \\ \langle F_{\bar{\alpha}} F_{\bar{\alpha}} \rangle &= \frac{s^2}{N} \left[2\eta m - \frac{1}{2}s^2 \frac{\bar{\alpha}}{\bar{\alpha}^+} \right]. \end{aligned} \quad (7.18)$$

These are exactly equivalent to our previous high-intensity solutions, the only difference being that the parameter s is now related to the pumping from the ground level to the upper lasing level, rather than the pumping rate from the lower to upper lasing level, as was the case in Ref. 1.

VIII. SIMULATION OF THE LASER EQUATIONS

If we set $X_0=1$ and $Z=0$ in the system of equations (6.5) and (6.6), then we are in the standard laser configuration which may be solved exactly using numerical simulation techniques. The first step is to write the noise terms $\Gamma_{\bar{x}}$ in (6.5) as a linear combination of independent white noises, with coefficients satisfying the correlation requirements of the diffusion matrix (6.6). As explained in Ref. 1, for a zero temperature reservoir (i.e., where $n, m, m^*=0$) this requires 12 noise terms

$$\begin{aligned} \Gamma_{\bar{\alpha}} &= \frac{s}{4N^{1/2}} (\bar{B} + \bar{D})(\xi_1 + i\xi_2) \\ &\quad - \frac{s}{2N^{1/2}} \bar{v} [(\xi_5 + i\xi_6) - (\xi_9 + i\xi_{10})], \\ \Gamma_{\bar{\alpha}^+} &= \frac{s}{4N^{1/2}} (\bar{B} + \bar{D})(\xi_3 + i\xi_4) \\ &\quad - \frac{s}{2N^{1/2}} \bar{v}^+ [(\xi_7 + i\xi_8) - (\xi_{11} + i\xi_{12})], \\ \Gamma_{\bar{v}} &= \frac{s}{N^{1/2}} (\xi_3 - i\xi_4), \quad \Gamma_{\bar{v}^+} = \frac{s}{N^{1/2}} (\xi_1 - i\xi_2), \\ \Gamma_{\bar{D}} &= \frac{s}{N^{1/2}} [(\xi_5 - i\xi_6) + (\xi_7 - i\xi_8)], \\ \Gamma_{\bar{B}} &= \frac{s}{N^{1/2}} [(\xi_9 - i\xi_{10}) + (\xi_{11} - i\xi_{12})]. \end{aligned} \quad (8.1)$$

We now write the system of stochastic equations in the general form

$$d\mathbf{x} = \mathbf{A}(\mathbf{x})dt + \underline{\mathbf{B}}(\mathbf{x}) \cdot d\mathbf{W}(t), \quad (8.2)$$

where $dW_i = \xi_i dt$, $\mathbf{A}(\mathbf{x})$ is the vector of deterministic parts from (6.5), and $\underline{\mathbf{B}}(\mathbf{x})$ is the noise matrix defined by (8.1).

The system (8.2) is integrated using the mixed implicit-explicit method of McNeil and Craig,⁶ which results in the difference equations

$$\begin{aligned} \Delta \mathbf{x}^n &= \mathbf{x}^{n+1} - \mathbf{x}^n \\ &= (1 - \theta_1 \underline{J}_A^n \Delta t) [\mathbf{A}(\mathbf{x}^n) \Delta t + \underline{B}(\mathbf{x}^n) \cdot \Delta \mathbf{W}^n], \end{aligned} \quad (8.3)$$

where

$$\underline{J}_A^n = \left. \frac{\partial \mathbf{A}}{\partial \mathbf{x}} \right|_{\mathbf{x}=\mathbf{x}^n} \quad (8.4)$$

is the Jacobian matrix of \mathbf{A} evaluated at each mesh point. For each time step t^n , $\Delta \mathbf{W}^n$ is evaluated as $\mathbf{Z}(n)(\Delta t)^{1/2}$, where $\mathbf{Z}(n)$ is a vector of random numbers from the distribution $N(0,1)$. The choice $\theta_1 = \frac{1}{2}$ is called “time centered” and has the best properties in terms of local accuracy and stability (see Refs. 6 and 7).

The simulations are then conducted by integrating individual trajectories from the same initial condition $\mathbf{x}(0)$, over a specified time interval 0 to t_{\max} , using the numerical algorithm (8.3). In the limit of a large number of trials, the ensemble average over the trajectories at each time step represents the time development of a phase-space variable.

Standard laser operation, as discussed in Sec. VII, is in the adiabatic elimination limit where $\eta \ll 1$. The equation for the cavity variable α is then

$$\dot{\alpha} = -\eta \bar{\alpha} \left(1 - \frac{C}{h + 4\eta \bar{\alpha}^\dagger} \right) + F_{\bar{\alpha}}, \quad (8.5)$$

where $h = (1 + 2\gamma')(1 + \gamma')$.

The usual semiclassical theory gives the stable stationary solutions

$$\begin{aligned} \bar{\alpha} &= 0, \quad C \leq h, \\ \bar{\alpha} \bar{\alpha}^\dagger &= \frac{1}{4}(C - h), \quad C \geq h. \end{aligned} \quad (8.6)$$

Threshold is thus defined for $C = h$, where in order to obtain a reasonable inversion [from (5.9)] we have $\gamma' \rightarrow 0$ so that $C \rightarrow 1$. Our procedure, therefore, is to fix $\eta = 0.1$ and then vary C in the range 0.2 to 2.0 to discover whether the simulations display the same characteristic laser behavior. The parameter s is no longer free, but is determined by the choice of C and η as

$$s = (C\eta)^{1/2}. \quad (8.7)$$

We begin with the laser fully pumped and the cavity in the vacuum state. That is, we have an initial condition of N atoms in the upper lasing level and no atoms in the lower lasing level. In terms of the scaled variables this becomes

$$\begin{aligned} \bar{\alpha}(0) &= \bar{\alpha}^\dagger(0) = 0, \\ \bar{v}(0) &= \bar{v}^\dagger(0) = 0, \\ \bar{D}(0) &= \bar{B}(0) = 1. \end{aligned} \quad (8.8)$$

To test the operation of the simulated laser we initially investigated two physical quantities of interest, the cavity intensity $I(t)$ and the second-order correlation function (with no introduced time delay in the average) $g^2(0)[t]$. These are defined as

$$\begin{aligned} I(t) &= \text{Re}[\langle \alpha^\dagger(t) \alpha(t) \rangle_{\text{ens}}] \\ &= \frac{N}{s^2} \text{Re}[\langle \bar{\alpha}^\dagger(t) \bar{\alpha}(t) \rangle_{\text{ens}}] \\ &= \frac{N}{C\eta} \text{Re}[\langle \bar{\alpha}^\dagger(t) \bar{\alpha}(t) \rangle_{\text{ens}}], \end{aligned} \quad (8.9)$$

$$\begin{aligned} g^2(0)[t] &= 1 + \text{Re} \left[\frac{\langle [\alpha^\dagger(t)]^2 [\alpha(t)]^2 \rangle_{\text{ens}}}{[\langle \alpha^\dagger(t) \alpha(t) \rangle_{\text{ens}}]^2} \right] \\ &= 1 + \text{Re} \left[\frac{\langle [\bar{\alpha}^\dagger(t)]^2 [\bar{\alpha}(t)]^2 \rangle_{\text{ens}}}{[\langle \bar{\alpha}^\dagger(t) \bar{\alpha}(t) \rangle_{\text{ens}}]^2} \right]. \end{aligned} \quad (8.10)$$

IX. SIMULATION RESULTS

A. The 10 000-atom laser

The first simulation we performed using the scheme of Sec. VIII was of a laser with an average number of 10 000 atoms in the upper lasing levels. The parameter γ' was set to be 0.01; this allows for a low level of lasing level transitions through mechanisms such as spontaneous emission and spurious pumping (i.e., atoms in the lower lasing level getting additional energy from some extra source to go to the upper level). Thus threshold for this system is at

$$C = h = 1.0302. \quad (9.1)$$

Representative results for $I(t)$ and $g^2(0)[t]$, in situations both above and below threshold, are shown in Figs. 3–6.

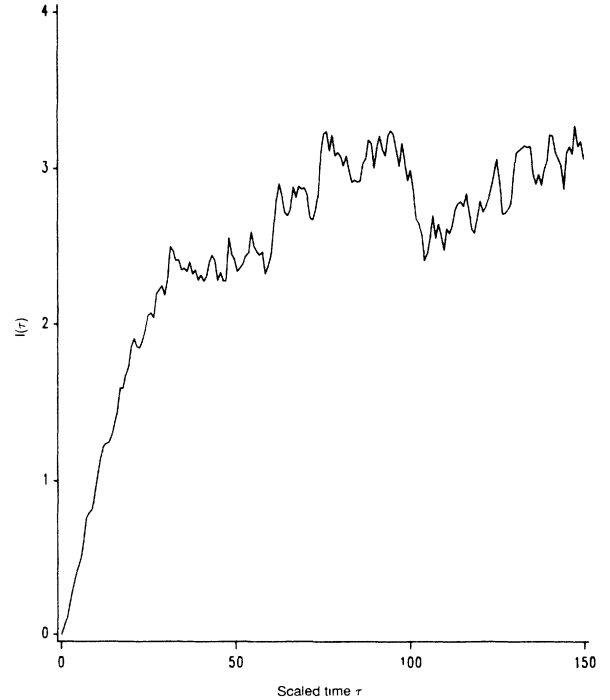


FIG. 3. Cavity intensity vs time, using full simulation parameters: $C = 0.8$, $N = 10\,000$, $dt = 0.05$, $\eta = 0.1$, $\gamma' = 0.01$, 1050 trials.

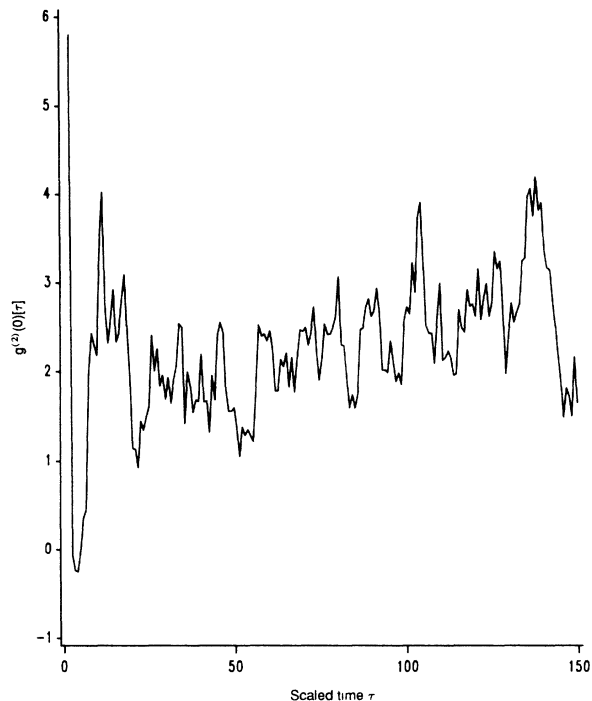


FIG. 4. Second-order correlation function vs time, using full simulation parameters: $C=0.8$, $N=10\,000$, $dt=0.05$, $\eta=0.1$, $\gamma'=0.01$, 1050 trials.

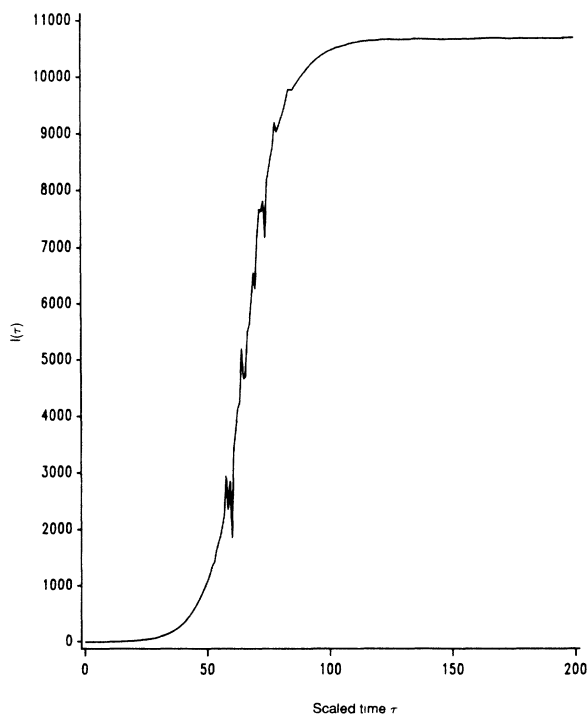


FIG. 5. Cavity intensity vs time, using full simulation parameters: $C=1.8$, $N=10\,000$, $dt=0.05$, $\eta=0.1$, $\gamma'=0.01$, 1100 trials.

The results above threshold are entirely as expected and clearly show the three regions of laser operation as defined by Haken.¹³ The first of these is the spontaneous-emission stage; this is characterized by very small fluctuations in the cavity intensity above the vacuum with $g^{(2)}(0)$ remaining around 2, the value for an incoherent light source. Region 2 is the stimulated emission stage, where the intensity of the spontaneous emission is amplified dramatically by induced emission. During this increase $g^{(2)}(0)$ has no fixed value and may fluctuate wildly. Finally, in region 3 we obtain saturation, the cavity intensity reaching a very stable stationary value. The second-order correlation function at the same time quickly settles to a value of 1, thus indicating the normal laser operation of a coherent intense light.

Below threshold, Figs. 3 and 4, the laser simulations all display the same time behavior. This essentially involves tending towards some stationary limit, the value of which is determined by the level of spontaneous-emission fluctuations.

If we choose the cooperativity parameter C to be close to threshold, then the laser simulations clearly display the phenomenon of critical slowing down. This is reflected in the time for the laser to reach saturation just above threshold (see Fig. 7 for $C=1.1$). Using a simplified deterministic analysis, the time constant for the threshold from region 1 to region 2 is given by

$$\chi = \frac{h}{2\eta(C-h)}. \quad (9.2)$$

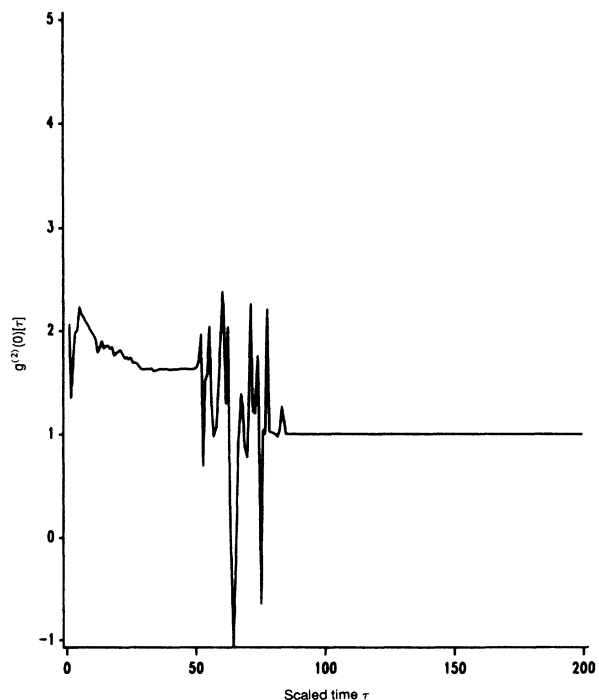


FIG. 6. Second-order correlation function vs time, using full simulation parameters: $C=1.8$, $N=10\,000$, $dt=0.05$, $\eta=0.1$, $\gamma'=0.01$, 1100 trials.

Therefore as $C \rightarrow h$, this time constant gets very large, and we get critical slowing down.

To provide a summary of the 10 000 atom laser, the stationary limits for the simulations are now plotted versus the cooperativity parameter (Figs. 8 and 9), together with the predictions for the semiclassical steady states. These results would seem to confirm the stationary behavior of the laser simulation both above and below threshold. The only slight discrepancy is very close to threshold where it is difficult to exactly obtain the stationary limit, but this is also the region where the potential solution is furthest away from the deterministic solution.

It is important to say, that in conducting this simulation, numerical spikes were experienced when simulating laser operation for a choice of C above threshold. However, these spikes only occurred during region 2, i.e., during the region of rapid intensity amplification. Thus if C is chosen below threshold, or if the initial cavity intensity corresponds to being in the saturation region, then the time development is without any spiking behavior.

If we analyze a single trajectory which experiences a spike, then the spike may be seen to correspond to an explosion of the trajectory into ten-dimensional phase space (the explosion is not into the full 12 dimensions—this is due to the last two dimensions describing the number of lasing atoms, which is constrained to vary around the average number). These spike trajectories are thus of the characteristic loop structure discussed in our previous pa-

per⁷ for a two-dimensional system. Extending this work in dimension, we can think of the laser equations becoming first-order unstable during the amplification process. Single trajectories may then be driven by the noise into

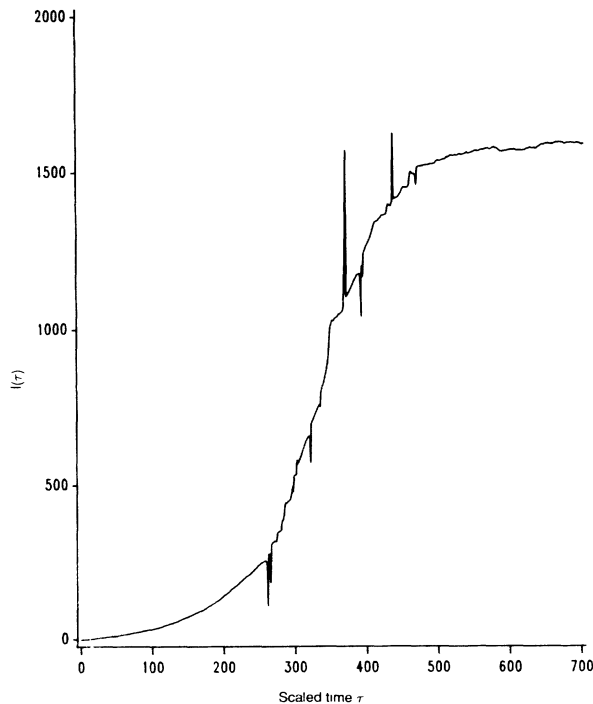


FIG. 7. Cavity intensity vs time, using full simulation parameters: $C = 1.1$, $N = 10\,000$, $dt = 0.05$, $\eta = 0.1$, $\gamma' = 0.01$, 1050 trials.

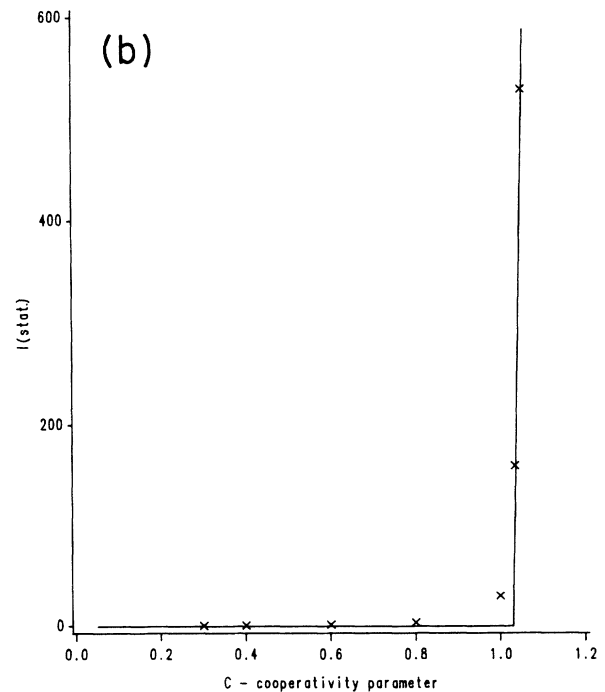
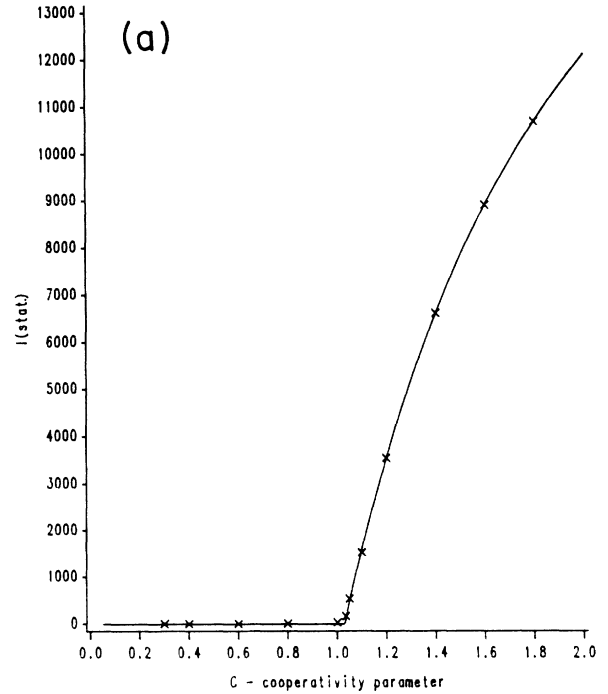


FIG. 8. Summary graphs—stationary intensity vs cooperativity parameter. —, semiclassical curve. \times , point obtained by simulations. Parameters: $N = 10\,000$, $dt = 0.05$, $\eta = 0.1$, $\gamma' = 0.01$.

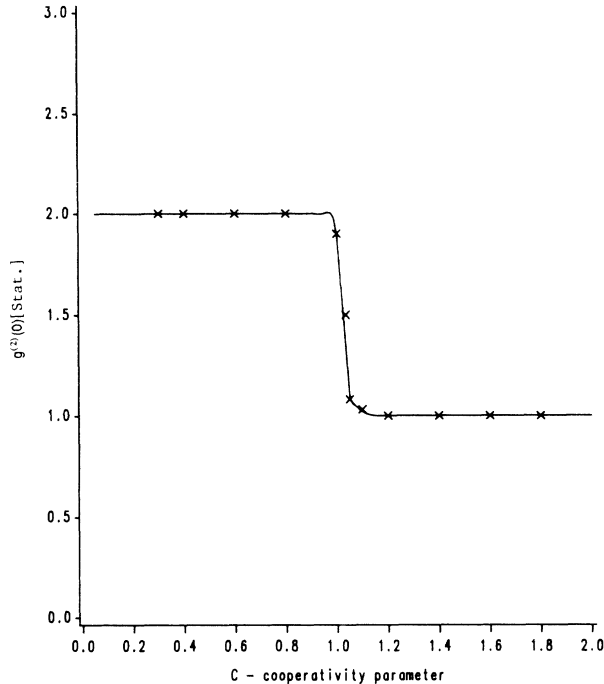


FIG. 9. Summary graph—stationary second-order correlation function vs cooperativity. —, potential solution curve. ×, point obtained by simulations. Parameters: $N = 10\,000$, $dt = 0.05$, $\eta = 0.1$, $\gamma' = 0.01$.

nonphysical portions of the extended phase space. The trajectory then embarks on a deterministically driven looped path in ten-dimensional phase space, causing the spike in the ensemble average, but must eventually return to the physical portion of phase space. For large values of the phase-space variables we would expect that the traditional Jaynes-Cummings terms dominate over the dissipative terms. This means that there are large oscillations in the trajectory, although the effect of the Jaynes-Cummings terms must be to keep the trajectory bounded.

In an infinite ensemble, the effect of these spike trajectories is averaged out over phase space and hence does not directly affect the time development of the system. However, in practical ensembles the spikes can mask the true behavior and since our numerical routines become inaccurate on the loop, we therefore remove trajectories from our averaging process if they reach a predetermined phase-space cutoff surface. The spikes which are present in Figs. 5–7 are the beginnings of spike trajectories which are then removed after exceeding the cutoff. Obviously, the negative spikes which appear in Fig. 6 are not physically allowable and so do not directly represent a physical situation. They are more likely to simply result from the use of finite ensemble sizes, as in an infinite ensemble there would always be a corresponding positive spike to cancel out the negative spike at any time point. However, this does not mean that the spikes have no physical relevance—indeed, the fact that the spikes all occur at the transition through threshold would suggest this.

One disturbing conclusion reached in Ref. 7 was that if there existed a finite probability of a spike in the stationary limit, then this signaled that the stationary time development could be suspect. In these simulations, however, despite the appearance of spikes, there seems no doubt that these simulations are indicating a time development for the laser which is in accordance with our physical expectations. At the very least, since the spikes are limited to a small part of the time development, outside this region we can be reasonably confident that the simulations are truly representing the nature of the exact laser equations.

B. The adiabatically eliminated laser

As a test of the results for our 10 000 atom laser we now proceed to simulate the set of adiabatically eliminated laser equations (8.5). The noise correlations are complicated in general, but provided we stay reasonably close to threshold we may then consider the small intensity approximation for the noise (with $n, m, m^* = 0$)

$$\langle F_{\alpha} F_{\alpha^+} \rangle = \frac{2s^4}{N(1+2\gamma')}, \quad \langle F_{\alpha} F_{\alpha} \rangle = 0 = \langle F_{\alpha^+} F_{\alpha^+} \rangle. \quad (9.3)$$

The simulations are generally conducted in a reduced four-dimensional phase space and two independent noise terms are required to represent (9.3). However, if the variables α and α^+ are chosen to be complex conjugate in

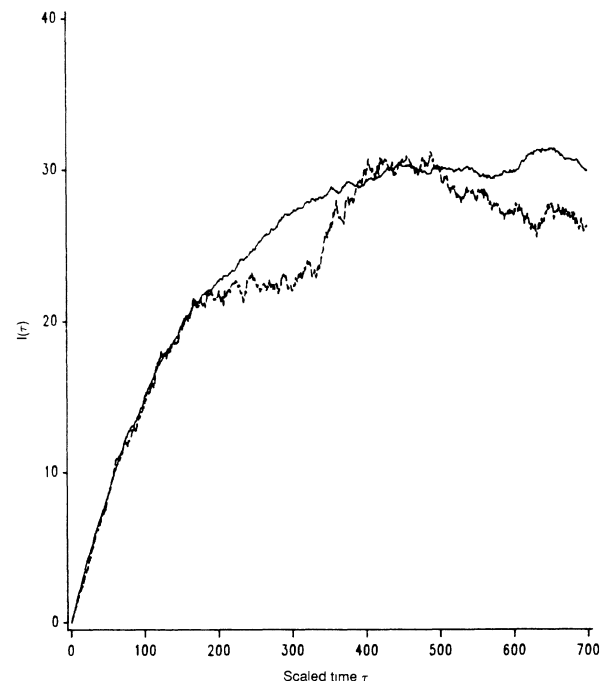


FIG. 10. Cavity intensity vs time, by two methods: —, adiabatic simulation, 4000 trials; --- full simulation, 1050 trials. Parameters: $C = 1$, $N = 10\,000$, $dt = 0.05$, $\eta = 0.1$, $\gamma' = 0.01$.

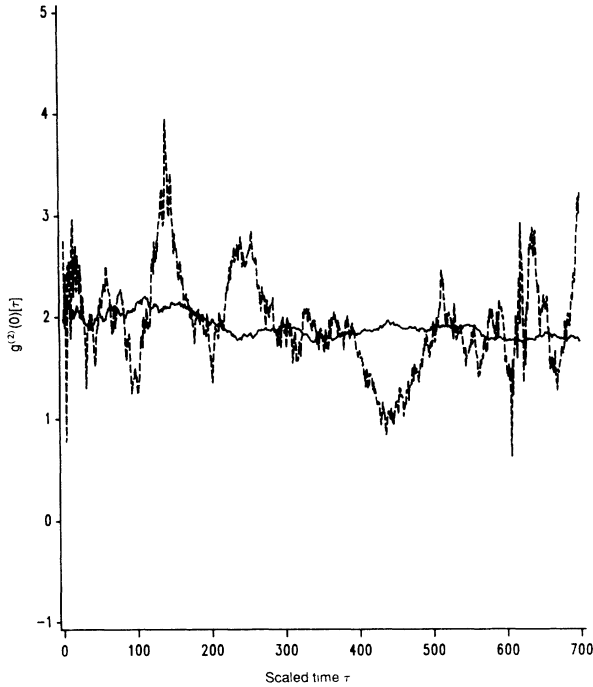


FIG. 11. Second-order correlation function vs time, by two methods: —, adiabatic simulation, 6000 trials; - - -, full simulation, 1050 trials, Parameters: $C=1$, $N=10000$, $dt=0.05$, $\eta=0.1$, $\gamma'=0.01$.

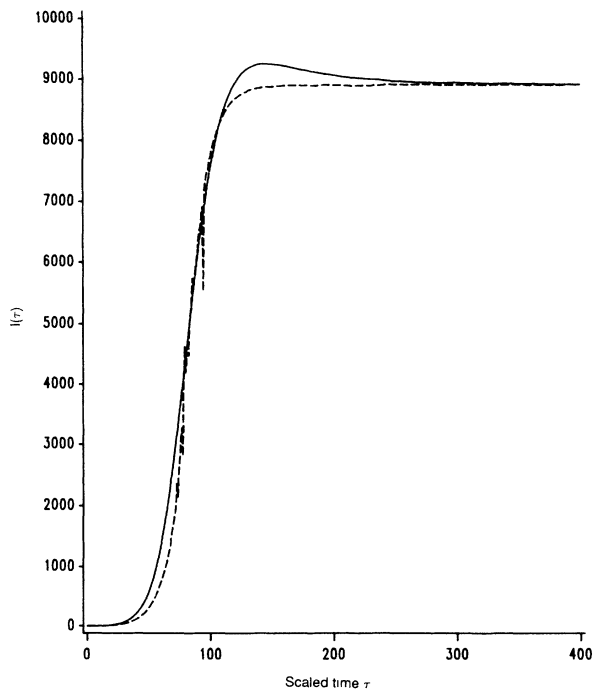


FIG. 12. Cavity intensity vs time, by two methods: —, adiabatic simulation; 6000 trials; - - -, full simulation, 1050 trials. Parameters: $C=1.6$, $N=10000$, $dt=0.05$, $\eta=0.1$, $\gamma'=0.01$.

the initial condition state, then the form of the equations will maintain the conjugacy and so we really only need to treat a two-dimensional phase space. This reflects the fact that for a constant noise term the positive- P representation collapses down to the standard Glauber-Sudarshan-Haken P function. Using an identical set of parameters to that in the full laser, simulations were performed of the adiabatically eliminated laser both above and below threshold (see Figs. 10–13). The results reinforce the nature of the time development of the simulations in Sec. IX A, displaying the same essential behaviors in saturation intensity, the time constant for laser amplification, and in critical slowing down.

At no point in these reduced system simulations, even during the rapid amplification phase, were any numerical spikes experienced. Hence no cutoff was required for the trajectories and all ensemble averages were obtained using all the trajectories. This extra stability is consistent with the assumptions involving the adiabatic elimination. This means that where a trajectory in the full simulation loops quickly out into the extended phase space, because the adiabatic elimination assumes a very slow cavity, then the trajectory in the reduced phase space has the instability smoothed out and hence no spike occurs.

The time development of the reduced laser system is not identical to that of the full laser system, but this is to be expected considering the simplicity of the noise term used in (9.3). However, the general characteristics are the same, which would seem to confirm that the full laser simulations in Sec. IX A are substantively correct.

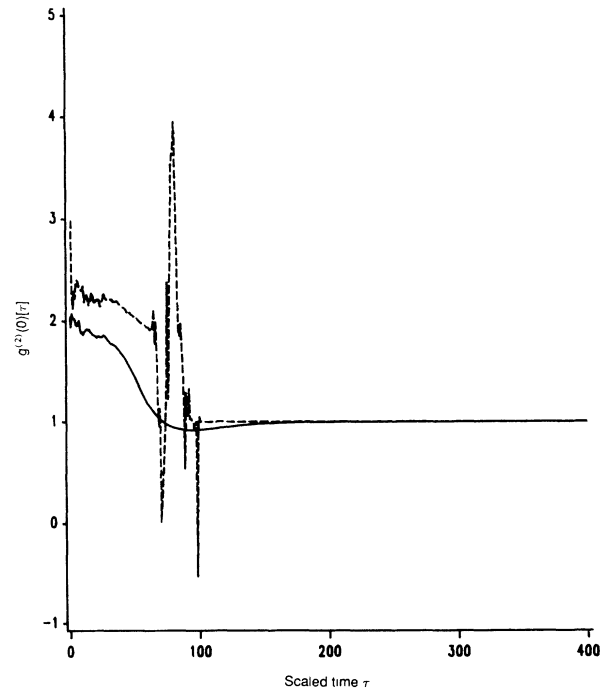


FIG. 13. Second-order correlation function vs time, by two methods: —, adiabatic simulation, 6000 trials; - - -, full simulations, 1050 trials. Parameters: $C=1.6$, $N=10000$, $dt=0.05$, $\eta=0.1$, $\gamma'=0.01$.

C. The few-atom laser

Since the stochastic laser equations have been reached without a scaling in the number of lasing atoms, then in principle they could be used to simulate a one-atom laser. The theoretical calculations in Sec. VII (and in our previous work¹) would suggest that this is possible provided that the parameter s is reduced in order to keep the quantum noise at a low level. As s is determined by C and η , this means that above threshold we require the cavity to be of extremely high quality, that is, we must have η ver small. However, by reducing η significantly, it can be seen from (9.2) that the time constant χ increases dramatically.

Thus, if we consider a one-atom laser with $\eta=0.0001$, then no laser operation is observed, or at least the simulation has not yet developed beyond the spontaneous-emission stage. That the simulation fails here, represents the fact that using a single lasing atom to produce laser light, although perfectly feasible from the equations, would require such a good cavity to catch and amplify the emissions, that a buildup to the coherent saturated laser output would be impossibly slow.

It may be possible to develop some kind of multiple time scale method to deal with this situation. The adiabatic elimination limit would seem to be appropriate at first glance, but in fact it requires n_s to be large, which is not necessarily the case in a one-atom laser.

However, a laser based on a small number of lasing atoms may still be constructed. If we set $N=100$ and $\eta=0.01$, then for $C=1.8$ the following time developments resulted (see Figs. 14 and 15). A saturated

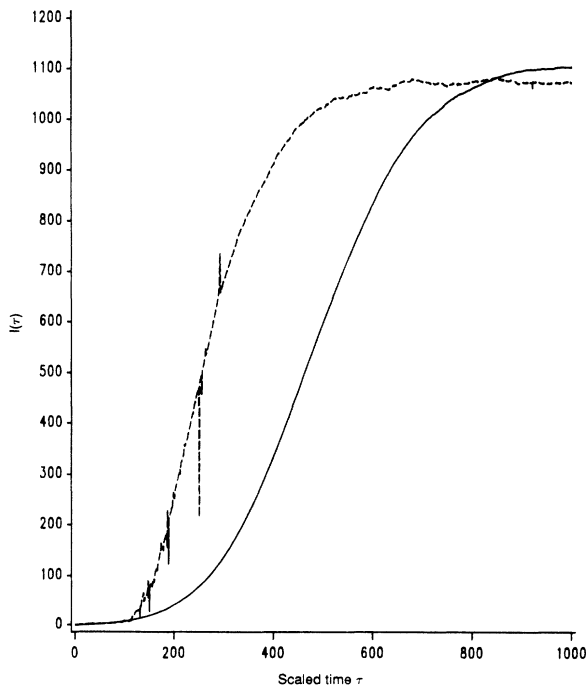


FIG. 14. Cavity intensity vs time, 100 atoms, by two methods: —, adiabatic simulation, 2000 trials; - - -, full simulation, 1000 trials. Parameters: $C=1.8$, $N=100$, $dt=0.05$, $\eta=0.01$, $\gamma'=0.01$.

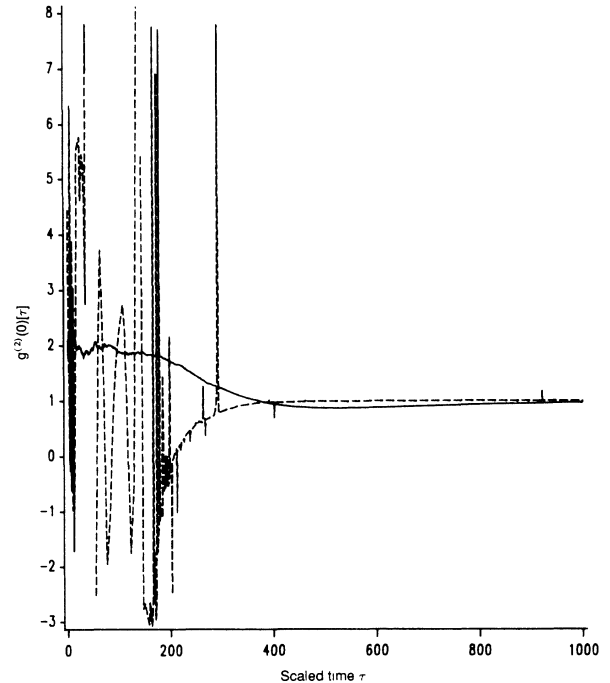


FIG. 15. Second-order correlation function vs time, 100 atoms, by two methods: —, adiabatic simulation, 2000 trials; - - -, full simulation, 1000 trials. Parameters: $C=1.8$, $N=100$, $dt=0.05$, $\eta=0.01$, $\gamma'=0.01$.

coherent laser output is now obtained, although the buildup is only achieved over a long time development. The time to reach amplification is about ten times that in our previous 10 000-atom simulation, a ratio consistent with (9.2) and the relative cavity quality factors.

In Fig. 15 we see huge fluctuations in the initial computation of $g^2(0)[t]$ which arise from very irregular behavior of the solutions in this region. These would presumably disappear with a sufficient number of trials. It is obvious that the simulation cannot be trusted in this region.

D. Two-time laser characteristics

All the simulations conducted thus far have involved the calculation of averages at single time steps in order to obtain information about the photon statistics, i.e., the intensity $I(t)$. However, it is perfectly possible to take ensemble averages where the variables are at two different time steps and hence reveal the nature of the laser spectrum.

The quantity that is normally calculated is the first-order correlation function $g^{(1)}(\tau, t)$, defined by

$$g^{(1)}(\tau, t) = \langle a^\dagger(t+\tau)a(t) \rangle = \langle \alpha^+(t+\tau)\alpha(t) \rangle, \quad (9.4)$$

or equivalently, its transform in Fourier space, called the laser spectrum

$$S(\omega, t) = \int_{-\infty}^{\infty} d\tau e^{-i\omega\tau} g^{(1)}(\tau, t). \quad (9.5)$$

If we now use our laser equations [both the full equations

(6.5) and the adiabatically eliminated equations (8.5)] to obtain simulation results for (9.4) and (9.5), then we may calculate the linewidth for the laser [defined as the half-width of (9.5) at half maximum] and compare it with analytical and experimental predictions. The simplest theory with which to check the simulation results, in the adiabatic elimination limit, is that arising from the reduced cavity equations, where we replace the stochastic term with a constant noise using approximation of Sec. VII A. Hence from (8.5) and (9.3)

$$d\tilde{\alpha} = -\eta\tilde{\alpha}f(\tilde{\alpha}\tilde{\alpha}^+)dt + \frac{1}{N^{1/2}}d\Gamma(t). \quad (9.6)$$

where

$$d\Gamma d\Gamma = 0 = d\Gamma^* d\Gamma^*, \quad d\Gamma d\Gamma^* = 2Qdt, \quad Q = \frac{s^4}{1+2\gamma'}. \quad (9.7)$$

The most obvious method for simulating two-time correlation functions would be to integrate the equations until we are in the stationary region and then fixing this time as t , continue the trajectory with τ and calculate the respective correlations. The ensemble average over the trajectories at each τ represents the time developments of the correlation function, and since we are in the stationary state this result should be independent of the starting time t .

However, provided the equations are ergodic⁴ we have the property of mean-square (MS) convergence:

$$\lim_{T \rightarrow \infty} \lim_{\text{MS}} \left[\frac{1}{T} \int_0^T dt x(t)x(t-\tau) \right]_{\text{one trial}} = [\langle x(t)x(t-\tau) \rangle_s]_{\text{ens}}. \quad (9.8)$$

We would expect stochastic equations to be ergodic in nearly all situations, and provided this condition is satisfied it is possible to construct an alternate method for simulating two-time correlations. We now require only a single trial, and at each time step calculate the products of the present value of a variable with variables at a previous set of τ steps. The trajectory is then advanced one time step and the correlation products recalculated. The results obtained from all the trajectory steps are then combined with averages taken over correlations with the same time difference τ . By (9.8) we should then correctly simulate the two-time stationary correlation function. The great advantage of this method is that it is much quicker than an ensemble average for two-time statistics, and in addition, we do not have to decide when a single trajectory is in the stationary region.

1. Below threshold, $C < h$

If we linearize (9.6) as $\alpha = \alpha_0 + \epsilon$, where $\alpha_0 = 0$, then to lowest order in ϵ we obtain

$$d\epsilon = -\eta\epsilon dt + \frac{1}{N^{1/2}}d\Gamma(t). \quad (9.9)$$

This can be written as an Ornstein-Uhlenbeck equation¹⁵

and hence has the stationary solution

$$\langle \alpha^+(t+\tau)\alpha(t) \rangle_s = \langle \epsilon^*(t+\tau)\epsilon(t) \rangle_s = \frac{Q}{\eta N} e^{-\eta|\tau|}. \quad (9.10)$$

Defining the correlation time as $\tau_c = 1/\eta$, then the stationary laser spectrum is given by

$$S(\omega) = \frac{Q}{\eta N} \int_{-\infty}^{\infty} d\tau \exp \left[- \left[i\omega\tau + \frac{|\tau|}{\tau_c} \right] \right] = \frac{2Q}{\eta N \tau_c} \frac{1}{\left[\frac{1}{\tau_c} \right]^2 + \omega^2}. \quad (9.11)$$

Simulations were now conducted in the below-threshold regime using the following parameter values: $C=0.3$, $\eta=0.1$, $\gamma'=0.01$, $N=10\,000$. The results for $g^{(1)}(t)$ and $S(\omega)$ obtained by simulating the adiabatically eliminated stochastic equations are shown in Figs. 16 and 17, together with the theoretical curves (9.10) and (9.11)

Both the correlation functions in Fig. 16 show the same basic exponential decay to zero within 10–15 corre-

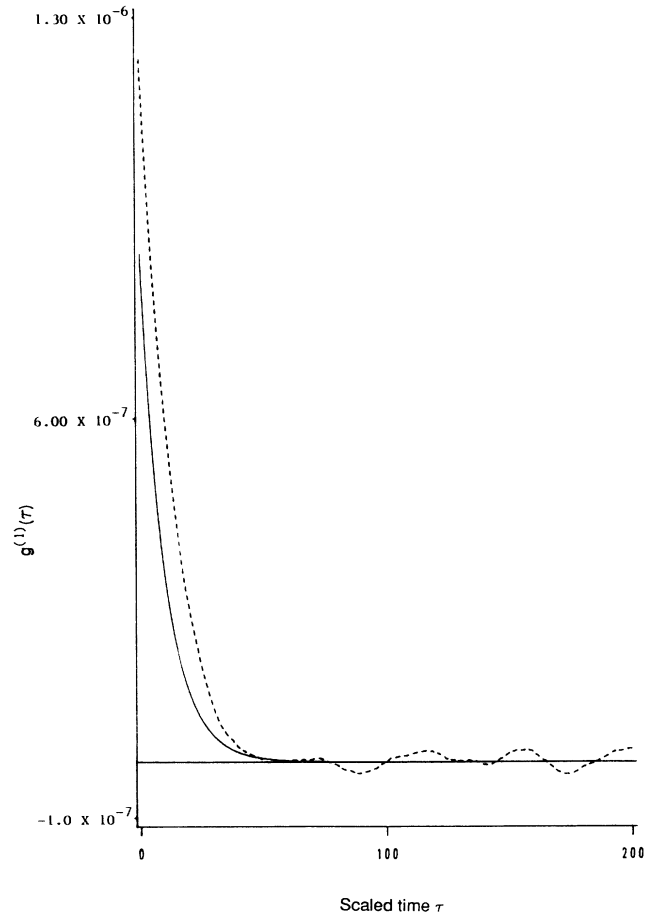


FIG. 16. First-order correlation function vs time. —, approximate theory. - - -, adiabatic simulation. Parameters: $C=0.3$, $n=10\,000$, $dt=0.05$, $\eta=0.1$, $\gamma'=0.01$, 300 000 trials.

lation times. The initial value for the adiabatic-eliminated curve (corresponding to the stationary variance) is exactly that predicted by the potential solution for the stationary situation.¹² In Fig. 17 the spectra have been normalized to the same maximum, and although the tail behaviors are slightly different, the linewidths obtained are almost identical. We may then conclude that (at least as far as the adiabatic-eliminated equations are concerned) the linearized theory below threshold correctly predicts an exponential dependence for the correlation function and an accurate figure for the laser linewidth. To check that our simulation procedure was in fact working correctly, we directly simulated the linearized equation (9.9). The correlation function thus obtained, after sufficient time steps, was almost exactly identical to the theoretical curve in Fig. 16. Further, when using an ensemble approach to simulating correlation functions we exactly reproduced the results in Fig. 16, therefore confirming the ergodic nature of the stochastic equations.

In the two-dimensional two-time simulations described thus far, averages over approximately 100 000 time events were required for convergence. We also attempted to evaluate correlation statistics in the full 12-dimensional

laser case. However, outside the first few correlation times, even for several million time events it proved impossible to sufficiently reduce the fluctuations in the results. It therefore appears that a much faster computer is required in order to accurately simulate the full laser equations.

2. Above threshold, $C > h$

The standard laser analysis above threshold in the adiabatic limit¹⁶ involves a change to amplitude and phase variables, as linearization is not valid directly in the α, α^+ basis. The stochastic equations that are finally obtained are, where $\alpha = R e^{i\phi}$,

$$dR = - \left[\eta R f(R^2) + \frac{Q}{2NR} \right] dt + \frac{1}{N^{1/2}} d\Gamma_R(t), \quad (9.12)$$

$$d\phi = \frac{1}{RN^{1/2}} d\Gamma_\phi(t), \quad (9.13)$$

with the correlations between the noises

$$d\Gamma_R d\Gamma_R = Q dt = d\Gamma_\phi d\Gamma_\phi, \quad d\Gamma_R d\Gamma_\phi = 0.$$

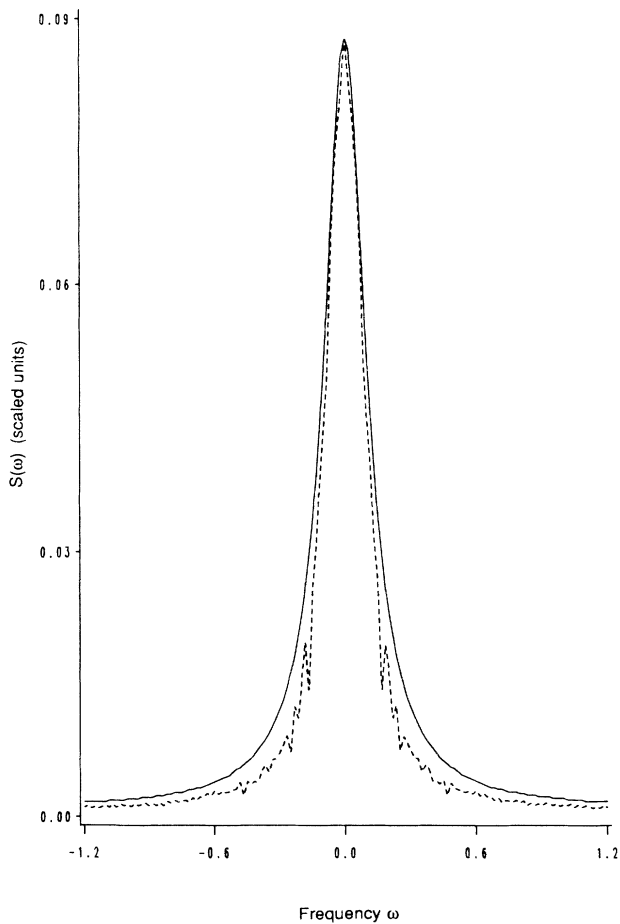


FIG. 17. Laser spectrum vs frequency. —, approximate theory. ---, adiabatic simulation. Parameters: $C=0.3$, $N=10\,000$, $dt=0.05$, $\eta=0.1$, $\gamma'=0.01$, 300 000 trials.

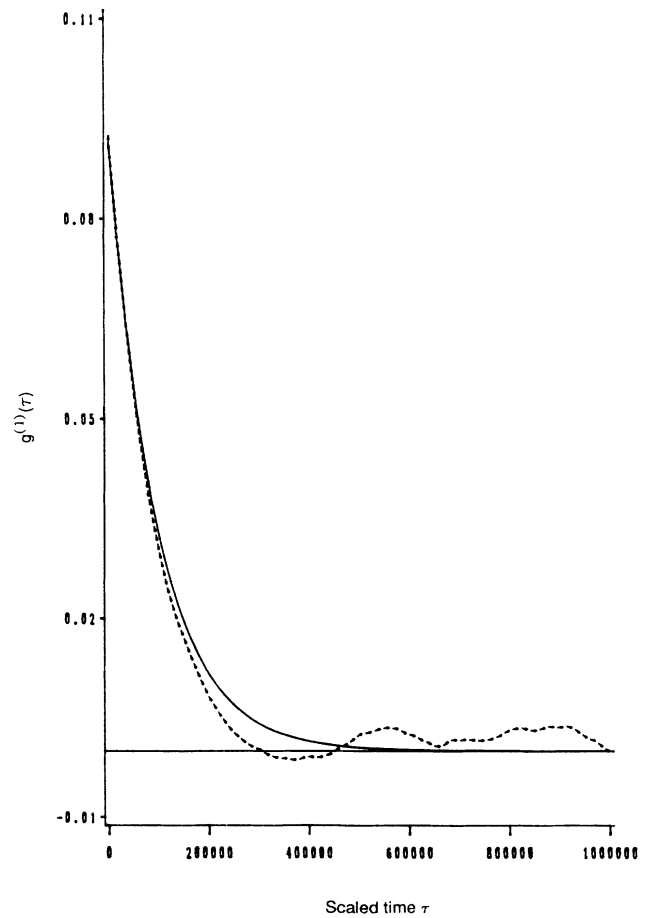


FIG. 18. First-order correlation function vs time. —, approximate theory. ---, adiabatic simulation. Parameters: $C=1.4$, $N=10\,000$, $dt=0.05$, $\eta=0.1$, $\gamma'=0.01$, 100 000 trials.

The equation for the phase ϕ , (9.13), thus exhibits the perfect phase diffusion characteristic of a laser operating above threshold.

To calculate the first-order correlation function

$$\langle \alpha^+(t+\tau)\alpha(t) \rangle = \langle R(t+\tau)R(t) \exp\{-i[\phi(t+\tau)-\phi(t)]\} \rangle, \quad (9.14)$$

we assume that for large N , the amplitude fluctuations are small and thus

$$R(t+\tau) = R(t) = R(\infty) = [\frac{1}{4}(C-h)]^{1/2}. \quad (9.15)$$

Hence we may integrate (9.13) and using the Gaussian nature of the noise obtain

$$\langle \alpha^+(t+\tau)\alpha(t) \rangle = \frac{1}{4}(C-h) \exp\left[-\frac{|\tau|}{\tau_c}\right]. \quad (9.16)$$

The correlation time is defined as $\tau_c = N(C-h)/2Q$ and results in the theoretical laser spectrum

$$S(\omega) = \frac{1}{2}(C-h) \frac{\tau_c}{\left[\frac{1}{\tau_c}\right]^2 + \omega^2}. \quad (9.17)$$

We would expect this model to become more accurate as we go further above threshold, where the phase fluctuations increasingly dominate. We thus make the choice of parameters $C=1.4$, $N=10\,000$, $\eta=0.1$, $\gamma'=0.01$ which results in a correlation time $\tau_c=96\,223.47$.

This very large value reflects the fact that with the very small noises we are using, the α vector takes a very long time to diffuse around the circular phase-space distribution and thus the laser linewidth is very narrow. Conducting simulations then becomes more difficult as we need to extend τ over a very large time interval in order to obtain the full correlation behavior. However, by calculating correlations at every 1000th step instead of every step, it is possible to obtain a reasonable picture of the phase diffusion. In Fig. 18 we show the simulation result for the correlation function obtained using the adiabatic-eliminated equations. The results confirm exactly the phase-diffusion process over the first 2–3 correlation times. The discrepancy that occurs for times longer than this is almost certainly not physical but it simply was not possible to run the simulation long enough to reduce the fluctuations at very long correlation times.

X. CONCLUSION

Although the use of three-level atoms in a laser model is not new (i.e., the laser models of Louisell and Gordon), in recent times the favored approach has been to use a two-level atom model to derive phase-space equations for the laser (following Haken). In our previous paper, we presented a new phase-space method for the two-level system involving a generalized P representation, but although an exact Fokker-Planck equation was obtained, there was an unexplained instability in the resultant stochastic equations.

To attempt to remove this instability, in this paper we considered again a three-level atom laser model. If the reasonable assumption was made that the ground level acts as an extra reservoir to the atoms in the lasing levels, then a stable system of stochastic differential equations was obtained in an extended phase space [see (6.5)]. These equations are exact, in the sense that there is no truncation of higher-order derivatives and thus have great potential in the solution of laser, optical bistability, and Jaynes-Cummings problems, for both small and large numbers of excited atoms.

The major method of analytic solution considered here has been in the adiabatic elimination limit, where leading noise terms have been calculated and resulted in simplified Fokker-Planck equations in certain regimes. For optical bistability, using methods described by Drummond and Walls,¹¹ linearized results may be obtained for the full adiabatically eliminated equations. A confirmation of their results is thus feasible and, in addition, a linearized theory of one-atom optical bistability is possible.

A second method of analytic solution, which is valid outside the range of adiabatic elimination, is to employ the method of linearization in frequency space as developed by Reid.¹⁷ The method was developed by Reid using a truncated Fokker-Planck equation, so that we would now have an extra dimension in the problem with our equations. However, due to the simplicity of the extra equation, the stability criteria to be satisfied are identical to that stated in Ref. 17. These will only be satisfied for optical bistability, but results may now be established in both the good and bad cavity limit.

All of these analytic methods have limitations in application and to solve fully nonlinear problems, we are thus required to look at numerical methods of solution. In this paper we have concentrated on the technique of direct simulation of the stochastic (Langevin) equations. For a laser configuration, we have performed simulations of the full set of laser equations (in the adiabatic elimination regime) and compared this with simulations of the simplest adiabatically eliminated equations. Although some numerical problems are experienced at threshold, the results showed all the features of laser operation and agreed entirely with our physical expectations. Future simulations are planned, in which the full system of equations are used to analyze the region where the parameter η is increased from the adiabatic elimination limit and thus observe the breakdown in standard laser operation.

Of course, numerical simulation techniques may be used for the equations in an optical bistability configuration, although we do not treat them in this present paper. Simulations have already been performed by Carmichael, Satchell, and Sarkar⁵ at the critical point, using stochastic equations obtained from a truncated Fokker-Planck equation. It would therefore be interesting to check whether their results may be replicated using our new equations.

In addition, since the system of equations (6.5) is in principle valid for a single excited atom, then we could simulate bistability on this small scale. Results here could be checked against the numerical calculations of

Savage and Carmichael,¹⁸ which showed that single atom bistability was possible for large saturation photon numbers.

Finally, it would be a simple matter to extend these

simulations to include an analysis of the Jaynes-Cummings problem, where we study the interaction between an undriven light mode and an ensemble of passive atoms.

¹A. M. Smith and C. W. Gardiner, *Phys. Rev. A* **38**, 4073 (1988).

²J. P. Gordon, *Phys. Rev.* **161**, 367 (1967).

³W. H. Louisell, *Quantum Statistical Properties of Radiation* (Wiley, New York, 1973); derivation in Markov approximation, pp. 335–368.

⁴P. D. Drummond and C. W. Gardiner, *J. Phys. A* **13**, 2353 (1980).

⁵H. J. Carmichael, J. S. Satchell, and S. Sarkar, *Phys. Rev. A* **34**, 3166 (1986).

⁶K. J. McNeil and I. D. S. Craig (unpublished).

⁷A. M. Smith and C. W. Gardiner, *Phys. Rev. A* **39**, 3511 (1989).

⁸W. H. Louisell, Ref. 3; see explanation of his three-level atom laser model beginning p. 469.

⁹R. Loudon, *The Quantum Theory of Light* (Clarendon, Oxford, 1973); see Fig. 10.4, p. 242.

¹⁰H. Haken, in *Licht und Materie*, Vol. XXV/2c of *Handbuch*

der Physik, edited by S. Flügge (Springer-Verlag, Berlin, 1970); this is the standard scaling for g ; see, for example, the scaling argument on p. 155.

¹¹P. D. Drummond and D. F. Walls, *Phys. Rev. A* **23**, 2563 (1981).

¹²M. D. Reid, K. J. McNeil, and D. F. Walls, *Phys. Rev. A* **24**, 2029 (1981).

¹³H. Haken, in Ref. 10; refer to diagram, p. 167.

¹⁴C. W. Gardiner, *Handbook of Stochastic Methods* (Springer-Verlag, Berlin, 1983); refer to pp. 57–60.

¹⁵C. W. Gardiner, Ref. 14; refer to pp. 106 and 107.

¹⁶M. Sargent, M. O. Scully, and W. E. Lamb, Jr., *Laser Physics* (Addison-Wesley, Reading, MA., 1974); see theory on pp. 335ff.

¹⁷M. D. Reid, *Phys. Rev. A* **37**, 4792 (1988).

¹⁸C. M. Savage and H. J. Carmichael, *IEEE J. Quantum Electron.* **24**, 1495 (1988).